

Levels of symmetry adapted perturbation theory (SAPT). II. Convergence of interaction energy components

Jeffrey B. Schriber,¹ Austin M. Wallace,¹ Daniel L. Cheney,² and C. David Sherrill^{1, a)}

¹⁾Center for Computational Molecular Science and Technology, School of Chemistry and Biochemistry, and School of Computational Science and Engineering, Georgia Institute of Technology, Atlanta, Georgia, 30332-0400, USA

²⁾Molecular Structure and Design, Bristol Myers Squibb Company, P.O. Box 5400, Princeton, New Jersey 08543, USA

(Dated: 11 April 2025)

Symmetry adapted perturbation theory (SAPT) is a valuable theoretical technique useful in quantifying intermolecular interaction energies in terms of four physically meaningful components: electrostatics, exchange-repulsion, induction/polarization, and London dispersion. We present a systematic analysis of the convergence of SAPT total and component energies with respect to level of theory and basis set using an extended database of 4569 van der Waals dimer geometries. Our analysis supports the use of SAPT0/aug-cc-pVDZ over previously recommended *s*SAPT0/jun-cc-pVDZ as an economical level of SAPT. Our previous recommendations of SAPT2+/aug-cc-pVDZ and SAPT2+(3) δ MP2/aug-cc-pVTZ as medium and high cost variants, respectively, remain unchanged. However, SAPT0/aug-cc-pVDZ and SAPT2+/aug-cc-pVDZ total interaction energies on average rely on error cancellations, so they should be used with caution when parameterizing SAPT-based force fields and intermolecular potentials. SAPT2+(3)/aug-cc-pVTZ shows quantitatively accurate component energies, making it the preferred choice for applications when feasible. Lastly, we examine a focal point approximation that approaches the accuracy of SAPT2+(3) δ MP2/aug-cc-pVTZ with a significantly reduced cost.

I. INTRODUCTION

Theoretical treatments of non-covalent intermolecular interactions have contributed much to our understanding of numerous chemical phenomena,^{1–3} including the formation of organic crystals,^{4,5} protein folding and ligand binding,^{6,7} and stacking of nucleic acids,^{8,9} to name a few. From a theoretical viewpoint, the most fundamental computable quantity to describe a non-covalent interaction is the interaction energy, which we define using the supermolecular approach,

$$E_{\text{int}}^{\text{AB}} = E^{\text{AB}} - (E^{\text{A}} + E^{\text{B}}), \quad (1)$$

where E^{AB} is the total energy of a weakly bound dimer complex and E^{A} and E^{B} are the total energies of the isolated monomers A and B. Interaction energies quantify the magnitude of a repulsive or attractive interaction between two molecular systems, though they do not give information about the underlying forces dictating the strength of the interaction. Here, we assume that monomers A and B keep the same internal geometry they have in the dimer AB; that is, monomer deformation contributions are not included in $E_{\text{int}}^{\text{AB}}$.

While computation of an intermolecular interaction energy is straightforward using the supermolecular approach, one needs to be careful when choosing the underlying computational method. Equation (1) combines computations on systems with different numbers of electrons, so size-consistent methods should be prioritized, in addition to methods that typically show good cancellation of errors. Accordingly, coupled cluster with singles, doubles, and perturbative triples [CCSD(T)],¹⁰ particularly when extrapolated to the complete

basis set limit (CBS), is considered the “gold standard” for interaction energies and the best accessible method for benchmarking more approximate theories.¹¹ The steep $\mathcal{O}(n^7)$ scaling of conventional CCSD(T) limits its application to small dimers, so significantly more economical approaches are needed in applications to large, biologically relevant interacting systems. Second-order Møller–Plesset perturbation theory (MP2) can be applied to much larger systems, though it is now well-known to overbind dimers exhibiting large dispersion-dominated interactions.¹² An elegant alternative is the regularized κ MP2 method of Lee et al.,^{13–15} which reduces error in intermolecular interaction energy with respect to MP2, with no change in computational cost. Even more economical solutions are based on a variety of dispersion-corrected density functional theory (DFT) approaches, most commonly the DFT-D methods of Grimme et al.^{16–22} The accuracy of DFT-D can be variable, though these methods can be applied to significant portions of protein-ligand systems and large host-guest complexes difficult to reach with conventional ab initio techniques.²³

Despite the successes of supermolecular approaches, they typically cannot provide insight to the underlying forces of the intermolecular interaction. Energy Decomposition Analysis (EDA) can be applied after a supermolecular interaction energy computation to obtain a breakdown of the interaction energy in terms of fundamental forces of intermolecular interactions, but the partitioning is not uniquely defined and so one obtains different breakdowns for different EDA methods.^{24–30} Rather than applying these decomposition schemes *a posteriori*, one can use an intermolecular perturbation theory to express the interaction energy with physically-meaningful terms. Symmetry-adapted perturbation theory (SAPT) defines monomer-centered, zeroth-order Hamiltonians and solves for the interaction energy perturbatively.^{31–33} Moreover, the inter-

^{a)}Electronic mail: sherrill@gatech.edu

action energy is written as a sum of terms naturally categorizable into one of four interaction components: electrostatics, exchange-repulsion, induction/polarization, and London dispersion. Electrostatics is the Coulombic interaction between the charge distributions of the isolated monomers. Exchange-repulsion is an always repulsive force arising from the anti-symmetry requirement of the dimeric wavefunction, and it can be thought of as the organic chemists' concept of steric repulsion. Induction is the polarization of each monomer in response to the electric field of the other monomer, and it is always attractive. Allowing for the correlation of electrons between monomers also leads naturally to an energy lowering contribution identifiable as London dispersion interactions.

At sufficiently high levels of SAPT theory, interaction energies are in good agreement with other high-level benchmarks, e.g., from CCSD(T).³⁴ Beyond this, however, SAPT components have been extremely useful in characterizing interactions in a variety of contexts,⁹ for example, by providing insight to specific interactions between drug-like molecules and protein targets.^{2,7,35} The energy components of SAPT have also been successfully used in developing highly accurate force fields and intermolecular potentials.^{36–46} SAPT also avoids several complications associated with the supermolecular approach, notably the aforementioned size-consistency errors and basis set superposition errors.

SAPT can be formulated in a variety of ways. The monomers can be treated at the Hartree–Fock level, and the intermolecular interaction and intramolecular correlation can be treated in a triple perturbation theory.^{31,47} This wavefunction-based SAPT has a variety of levels depending on the inter- and intra-molecular perturbation orders. Stopping at second order in the intermolecular perturbation and neglecting intramolecular correlation yields a method called SAPT0 and is one of the most common choices due to its relatively low computational cost. While the accuracy of SAPT0 can be reasonable given a careful choice of basis set,^{34,48} several improvements have been developed to reach quantitative accuracy without increasing the cost. For example, replacing the HF treatment of monomers with density functional theory can greatly improve interaction energies if the treatment of dispersion is also updated (because the HOMO-LUMO gap is typically reduced in Kohn-Sham DFT, making the MP2-like treatment of dispersion from SAPT0 unsuitable in this context); the resulting approach is labeled SAPT(DFT) or DFT-SAPT.^{36,49–56} Empirical corrections to the dispersion component have also resulted in SAPT variants with favorable accuracy/cost ratios, based on SAPT0,^{57–59} SAPT(DFT),^{60,61} or extended SAPT (XSAPT).^{62–66} One implementation of SAPT0-D made use of graphics processing units and was able to be applied to the entire indinavir/HIV-II protease complex.⁵⁷ Alternatively, we recently reported⁶⁷ charge embedding extensions, like those used in mixed quantum mechanics / molecular mechanics (QM/MM) approaches, to SAPT0 and SAPT0-D, which are also capable of handling large complexes like ligands interacting with entire proteins.

Our prior work³⁴ examined the balance between cost and accuracy for a variety of levels of SAPT, focusing exclusively on total interaction energies. Due in part to a relatively small

dataset and limited SAPT data in quadruple- ζ basis sets, a clear “best” SAPT level could not be identified among those tested, though we did recommend several useful levels with generally favorable cost/accuracy ratios. A primary motivation of the present work is to re-examine the reliability of total interaction energies of the levels of SAPT using a dataset that is much larger and that features more results computed using quadruple- ζ basis sets. The present dataset includes more dimers featuring interactions typical of those found in biology, including halogen-containing dimers, dimers with non-zero net charge, and dimers with diverse interaction profiles computed along potential energy curves.

Importantly, we also extend the analysis to the performance of the interaction energy components. A better understanding of component accuracy will certainly aid in applications of SAPT to chemical problems, and it also provides some crucial guidance for selecting a reference theory in developing high-level, SAPT-based force fields and intermolecular potentials.^{36–46} Newer, SAPT-based force fields fit functional forms directly to SAPT component energies, though the choice of reference theory is typically guided by a combination of cost considerations and the accuracy in total interaction energy of the corresponding SAPT level. By analyzing both total and component interaction energies, we are additionally able to provide insight into the extent of error cancellations in SAPT and identify SAPT level and basis set combinations for which total and component interaction energies are reliable. We also perform a study of the convergence of the component energies with respect to both SAPT method and basis set. Lastly, we consider a focal point technique^{68,69} to improve the accuracy of the dispersion component in wavefunction-based SAPT without significantly increasing cost.

II. THEORY AND METHODOLOGY

A. SAPT

SAPT is a family of ab initio methods that directly compute the intermolecular interaction energy of a molecular dimer. In all SAPT methods, the dimeric Hamiltonian, \hat{H} is defined as a sum of zeroth-order Hamiltonians for each monomer with an intermolecular interaction operator,

$$\hat{H} = \hat{H}_A + \hat{H}_B + \hat{V}, \quad (2)$$

where A and B refer to each monomer and \hat{V} describes interactions between electrons and nuclei of one monomer with those of the other monomer, without the use of the supermolecular approach in Equation (1). In this work, we focus on wavefunction-based SAPT in which each monomeric zeroth-order Hamiltonian is the monomer's Fock operator, and to correct for intramonomer electron correlation, we add the Møller–Plesset fluctuation potential (\hat{W}), describing intramolecular electron correlation, as an additional perturbation for each monomer,

$$\hat{H} = \hat{F}_A + \hat{F}_B + \xi(\hat{W}_A + \hat{W}_B) + \lambda\hat{V}, \quad (3)$$

where ξ and λ represent intramolecular and intermolecular perturbation strengths, respectively. With this Hamiltonian, we can then write a SAPT interaction energy as a perturbation series written using the Rayleigh-Schrödinger type terms, E_{RS} , and exchange terms, E_{exch} ,

$$E_{\text{int}}^{\text{SAPT}} = \sum_{v=1}^{\infty} \sum_{w=0}^{\infty} (E_{\text{RS}}^{(vw)} + E_{\text{exch}}^{(vw)}), \quad (4)$$

where v specifies the perturbation order in V , and w specifies the sum of the perturbation orders in W_A and W_B .³¹ These Rayleigh-Schrödinger terms are typically attractive, while the exchange terms are always repulsive and arise from the antisymmetry requirement of the wave function with respect to electron exchange between monomers.

Varying inter- and intra-monomer perturbation orders yields a variety of levels of SAPT. In defining the levels of SAPT, we follow convention by relabeling Rayleigh-Schrödinger and exchange terms using their corresponding interaction energy type. The four main interaction types are electrostatics, exchange-repulsion, induction, and dispersion, though higher perturbation orders will lead to increasingly complicated cross terms combining two or more of these four types. In defining an interaction energy term, we always keep the superscript v and w labels, in addition to grouping terms in brackets whose sum is collectively assigned as one of the four interaction types.

Our group has developed efficient algorithms based on density fitting to implement various levels of wavefunction-based SAPT, described below, including terms through second order in v and w , and some third-order terms.^{35,70–73} These levels of SAPT are the ones examined in the present work. Our implementation has been made freely available in the open-source quantum chemistry program Psi4.⁷⁴ Our density-fitting adaptation and algorithms were based upon detailed equations for the individual SAPT terms taken from Refs. 75–77.

1. SAPT0 and *s*SAPT0

The simplest SAPT method, SAPT0, is defined as being second-order in v , and zeroth-order in w ,

$$\begin{aligned} E_{\text{int}}^{\text{SAPT0}} = & [E_{\text{elst}}^{(10)}]_{\text{elst}} + [E_{\text{exch}}^{(10)}]_{\text{exch}} \\ & + [E_{\text{ind},r}^{(20)} + E_{\text{exch-ind},r}^{(20)} + \delta E_{\text{HF}}^{[2]}]_{\text{ind}} \\ & + [E_{\text{disp}}^{(20)} + E_{\text{exch-disp}}^{(20)}]_{\text{disp}}. \end{aligned} \quad (5)$$

Detailed equations for each particular term can be found in Refs. 75 and 73. In Equation (5), we use a supermolecular Hartree-Fock (HF) correction, $\delta E_{\text{HF}}^{[2]}$. For SAPT methods that are second-order in v , some higher-order effects (primarily induction-like) can be implicitly captured by including the Hartree-Fock interaction energy, $E_{\text{int}}^{\text{HF}}$, computed according to Equation (1). Specifically, we define a HF correction appropriate for use with SAPT at second-order in v as the difference between the (counterpoise-corrected) HF interaction energy and a dispersion-less SAPT interaction energy with $v = 2$ and

$w = 0$,

$$\begin{aligned} \delta E_{\text{HF}}^{[2]} = & E_{\text{int}}^{\text{HF}} - ([E_{\text{elst}}^{(10)}]_{\text{elst}} + [E_{\text{exch}}^{(10)}]_{\text{exch}} \\ & + [E_{\text{ind},r}^{(20)} + E_{\text{exch-ind},r}^{(20)}]_{\text{ind}}). \end{aligned} \quad (6)$$

Throughout this work, we always include a δE_{HF} correction in computing interaction energies, and we associate it with the induction component, as it is expected to correspond primarily (but not exclusively) to higher-order induction effects.⁷⁸ Lastly, terms with the additional r subscript indicate the inclusion of orbital relaxation effects due to the other monomer, with the orbital response solved by the coupled perturbed HF equations. All orders of exchange-induction terms require this relaxation, in addition to electrostatic terms that include intra-monomer correlation.

Because of our use of a δE_{HF} correction, Equation (5) could also be written

$$E_{\text{int}}^{\text{SAPT0}} = E_{\text{int}}^{\text{HF}} + [E_{\text{disp}}^{(20)} + E_{\text{exch-disp}}^{(20)}]_{\text{disp}}, \quad (7)$$

which is simply a dispersion-corrected HF interaction energy. SAPT0 is the most computationally efficient SAPT level, particularly in its density-fitted implementation,^{35,71} and it has a cost similar to DF-MP2. However, SAPT0 neglects all intra-monomer correlation ($w = 0$), so its accuracy is expected to be limited.

Though we leave details to previous work,⁷⁵ $E_{\text{exch-ind},r}^{(20)}$ and $E_{\text{exch-disp}}^{(20)}$ are solved approximately using a formulation based on the square of the intermonomer orbital overlap, known as the single-exchange or S^2 approximation. This approximation is known to fail at short range, and additional scalings of these terms is common, often with empirical parameters. Originally, our implementation of SAPT scaled all terms invoking the S^2 approximation by the ratio

$$p_{\text{EX}}(\alpha) = \left(\frac{E_{\text{exch}}^{(10)}}{E_{\text{exch}}^{(10)}(S^2)} \right)^{\alpha}, \quad (8)$$

where $E_{\text{exch}}^{(10)}$ is the first-order exchange evaluated without the S^2 approximation, $E_{\text{exch}}^{(10)}(S^2)$ is the same term evaluated using the S^2 approximation, and the exponent α was set to 1. However, as pointed out by Schäffer and Jansen,⁷⁹ the ratios $E_{\text{exch}}^{(1)}(S^2)/E_{\text{exch}}^{(1)}$, $E_{\text{exch-ind}}^{(2)}(S^2)/E_{\text{exch-ind}}^{(2)}$, and $E_{\text{exch-disp}}^{(2)}(S^2)/E_{\text{exch-disp}}^{(2)}$ evaluated in DFT-based SAPT are not particularly close to each other, and hence scaling all S^2 -approximated terms by the same ratio is not well justified. In 2016, such scaling was turned off by default in our SAPT implementation in Psi4. However, in previous work³⁴ we found empirically that for very close contacts, results at the SAPT0 level were often improved using a “scaled” SAPT0 (*s*SAPT0) that scaled $E_{\text{exch-ind},r}^{(20)}$ and $E_{\text{exch-disp}}^{(20)}$ by $p_{\text{EX}}(3)$ (while leaving $\delta E_{\text{HF}}^{[2]}$ unchanged from its SAPT0 value).^{80,81}

2. SAPT2, SAPT2+, SAPT2+(3), and SAPT2+3

The first improvement to SAPTO that we will discuss was introduced by Misquitta et al.,⁸² where intramolecular correlation is included in electrostatics, exchange, and induction terms through $w = 2$. This method, named SAPT2, only improves upon these three components and not dispersion, making it asymptotically equivalent to supermolecular MP2. The SAPT2 interaction energy is

$$\begin{aligned} E_{\text{int}}^{\text{SAPT2}} = & [E_{\text{elst}}^{(10)} + E_{\text{elst,r}}^{(12)}]_{\text{elst}} \\ & + [E_{\text{exch}}^{(10)} + E_{\text{exch}}^{(11)} + E_{\text{exch}}^{(12)}]_{\text{exch}} \\ & + [E_{\text{ind,r}}^{(20)} + E_{\text{exch-ind,r}}^{(20)} + {}^t E_{\text{ind}}^{(22)} + {}^t E_{\text{exch-ind}}^{(22)} + \delta E_{\text{HF}}^{[2]}]_{\text{ind}} \\ & + [E_{\text{disp}}^{(20)} + E_{\text{exch-disp}}^{(20)}]_{\text{disp}}. \end{aligned} \quad (9)$$

Here the superscript t in ${}^t E_{\text{ind}}^{(22)} + {}^t E_{\text{exch-ind}}^{(22)}$ indicates that these terms are “true correlation” contributions⁸³ lacking any orbital response effects already captured by $E_{\text{ind,r}}^{(20)} + E_{\text{exch-ind,r}}^{(20)}$. Additional details about the individual terms involved in SAPT2 are provided in the literature.^{73,75,76,82,84}

SAPT2 can be improved by including the missing dispersion terms through $w = 2$, resulting in the SAPT2+ method.⁷⁰ The SAPT2+ interaction energy can be written compactly using the SAPT2 interaction energy,

$$E_{\text{int}}^{\text{SAPT2+}} = E_{\text{int}}^{\text{SAPT2}} + [E_{\text{disp}}^{(21)} + E_{\text{disp}}^{(22)}]_{\text{disp}}, \quad (10)$$

where $E_{\text{disp}}^{(22)}$ can be written⁷⁵ with the triples term separated from the singles, doubles, and quadruples term as $E_{\text{disp}}^{(22)} = E_{\text{disp}}^{(22)}[\text{SDQ}] + E_{\text{disp}}^{(22)}[\text{T}]$. The addition of this term causes SAPT2+ to behave similarly to MP4, with the notably expensive $\mathcal{O}(n^7)$ perturbative triples component of $E_{\text{disp}}^{(22)}$. The cost of computing $E_{\text{disp}}^{(22)}[\text{T}]$ can be drastically reduced with negligible effect on accuracy by using a basis of semicanonical MP2 natural orbitals and truncating this basis significantly (by up to half when using aug-cc-pVDZ).⁸⁵ By performing an identical truncation with $E_{\text{disp}}^{(20)}$ to produce an approximate $E_{\text{disp,approx}}^{(20)}$, we can accurately estimate the value of what $E_{\text{disp}}^{(22)}[\text{T}]$ would be without truncation if we apply the scaling factor $E_{\text{disp,exact}}^{(20)}/E_{\text{disp,approx}}^{(20)}$. Throughout this work, we always apply this scaling and natural orbital truncation with an occupation cutoff of 10^{-6} electrons (this is the default behavior in Psi4).

The next logical improvement to SAPT2+ is to include third order terms. Detailed equations can be found in Refs. 77 and 73. Rather than including all such third-order terms, SAPT2+(3) includes only partial third order effects beyond SAPT2+,⁷⁰

$$E_{\text{int}}^{\text{SAPT2+(3)}} = E_{\text{int}}^{\text{SAPT2+}} + [E_{\text{elst,r}}^{(13)}]_{\text{elst}} + [E_{\text{disp}}^{(30)}]_{\text{disp}}, \quad (11)$$

where notably $E_{\text{exch-disp}}^{(30)}$ is ignored due to its steep $\mathcal{O}(n^7)$ scaling. Interestingly, $E_{\text{disp}}^{(30)}$ has a scaling of $\mathcal{O}(n^6)$, which is formally less than the triples term already in SAPT2+, making SAPT2+(3) only marginally more expensive than SAPT2+.

SAPT2+3 (Ref. 86) builds on SAPT2+(3) by including higher-order induction and by appropriately including the coupling between dispersion and induction, exchange, and exchange-induction that occurs for $v = 3$,

$$\begin{aligned} E_{\text{int}}^{\text{SAPT2+3}} = & E_{\text{int}}^{\text{SAPT2+(3)}} \\ & + [E_{\text{exch-disp}}^{(30)} + E_{\text{ind-disp}}^{(30)} + E_{\text{exch-ind-disp}}^{(30)}]_{\text{disp}}. \end{aligned} \quad (12)$$

In addition, at the SAPT2+3 level, we explicitly compute the third-order induction and exchange-induction contributions $E_{\text{ind,r}}^{(30)} + E_{\text{exch-ind,r}}^{(30)}$. However, these contributions are already part of the supermolecular Hartree–Fock interaction energy correction $\delta E_{\text{HF}}^{[2]}$ term defined above. Thus, for SAPT2+3, we redefine the δE_{HF} correction as

$$\begin{aligned} \delta E_{\text{HF}}^{[3]} = & E_{\text{int}}^{\text{HF}} - ([E_{\text{elst}}^{(10)}]_{\text{elst}} + [E_{\text{exch}}^{(10)}]_{\text{exch}} \\ & + [E_{\text{ind,r}}^{(20)} + E_{\text{exch-ind,r}}^{(20)} + E_{\text{ind,r}}^{(30)} + E_{\text{exch-ind,r}}^{(30)}]_{\text{ind}}). \end{aligned} \quad (13)$$

This definition allows us to avoid double-counting the effect of $E_{\text{ind,r}}^{(30)}$ and $E_{\text{exch-ind,r}}^{(30)}$. The total “induction” term in SAPT2+3 is thus

$$\begin{aligned} E_{\text{ind}}^{\text{SAPT2+3}} = & E_{\text{ind,r}}^{(20)} + E_{\text{exch-ind,r}}^{(20)} + {}^t E_{\text{ind}}^{(22)} \\ & + {}^t E_{\text{exch-ind}}^{(22)} + E_{\text{ind,r}}^{(30)} + E_{\text{exch-ind,r}}^{(30)} + \delta E_{\text{HF}}^{[3]}. \end{aligned} \quad (14)$$

However, due to the inclusion of δE_{HF} , this actually gives the same overall induction contribution as SAPT2+(3); the benefit is that the contributions of $E_{\text{ind,r}}^{(30)}$ and $E_{\text{exch-ind,r}}^{(30)}$ are now explicitly available. In this work, we always include $\delta E_{\text{HF}}^{[3]}$, as it includes induction and exchange-induction effects beyond third-order. However, δE_{HF} also can produce spurious exchange effects, and in certain cases (particularly for nonpolar systems) pure SAPT induction (plus exchange-induction) through third order may be preferred over using $\delta E_{\text{HF}}^{[3]}$.⁷⁸

For levels of SAPT beyond SAPT2, we can apply an additional correction, denoted δMP2 , based on a supermolecular MP2 interaction energy, $E_{\text{int}}^{\text{MP2}}$,

$$\delta E_{\text{MP2}}^{[2]} = E_{\text{int}}^{\text{MP2}} - E_{\text{int}}^{\text{SAPT2}}, \quad (15)$$

$$\delta E_{\text{MP2}}^{[3]} = E_{\text{int}}^{\text{MP2}} - E_{\text{int}}^{\text{SAPT2}} - E_{\text{ind-disp}}^{(30)} - E_{\text{exch-ind-disp}}^{(30)}, \quad (16)$$

where $\delta E_{\text{MP2}}^{[2]}$ may be applied to SAPT2+ and SAPT2+(3) (resulting in SAPT2+ δMP2 and SAPT2+(3) δMP2), and $\delta E_{\text{MP2}}^{[3]}$ may be applied to SAPT2+3 (resulting in SAPT2+3 δMP2). Since MP2 and SAPT2 both by definition treat the intermolecular interaction energy to second order, the $\delta E_{\text{MP2}}^{[2]}$ correction is expected to include coupling between SAPT terms missing at the SAPT2 level. For SAPT methods that explic-

itly compute $E_{\text{ind-disp}}^{(30)} - E_{\text{exch-ind-disp}}^{(30)}$, we remove this from $\delta E_{\text{MP2}}^{[2]}$ and use instead $\delta E_{\text{MP2}}^{[3]}$ because we expect induction-dispersion coupling to be captured already in the supermolecular MP2 computation.³¹ Note that the SAPT2+δMP2 total interaction energy can be viewed as a supermolecular MP2 energy corrected by additional dispersion terms, similar to the approach used in MP2C.⁸⁷

Because the $\delta E_{\text{MP2}}^{[2]}$ correction is essentially a correction to recover coupling between terms, it doesn't easily fit into one of the four interaction types. As such, $\delta E_{\text{MP2}}^{[2]}$ and $\delta E_{\text{MP2}}^{[3]}$ are not assigned to any of the four components in the present work because the choice is unclear. This is a departure from our earlier work,³⁴ in which we assigned δE_{MP2} as "induction," expecting that the use of relaxed orbitals in the dimer computation of the supermolecular MP2 interaction energy would capture some of the same effects as correlation-dependent induction terms and cross terms. However, because the shape of the molecular orbitals is also governed by exchange effects, they could also be important in the supermolecular computation. In Figs. S29-S30 of the Supplemental Material, we present correlation plots between δE_{HF} , δE_{MP2} , and the four energy components from SAPT2+3, computed in the aug-cc-pVDZ and aug-cc-pVTZ basis sets, for the dataset considered in this work. $\delta E_{\text{HF}}^{[2]}$ is highly correlated with induction, which might be taken as data supporting its assignment as induction. On the other hand, the δE_{MP2} terms correlate much better with exchange than induction. This could be taken as an argument to assign them to exchange, but we simply leave them unassigned in the present work.

Finally, one additional improvement to SAPT2+, SAPT2+(3), and SAPT2+3 that we use here is to use coupled-cluster doubles (CCD) in computing all second-order dispersion terms. Specifically, one can apply the CCD+ST(CCD) method for computing intermolecular dispersion introduced by Williams et al.,⁴⁷ within a SAPT context. This technique uses CCD to compute monomer wavefunctions, from which dispersion amplitudes can be derived.⁸⁸ The monomer wavefunctions and the dispersion amplitudes are iteratively relaxed, and perturbative corrections to the dispersion energy from single and triple excitations are also included. What results is an iterative $\mathcal{O}(n^6)$ method that treats two-body correlations to infinite order. Previous work has combined CCD+ST(CCD) with virtual space orbital truncations, enabling computations on systems with as many as 30 atoms.⁷² We can then define the dispersion component for SAPT2+(CCD),

$$\begin{aligned} E_{\text{disp}}^{\text{SAPT2+}(CCD)} = & E_{\text{exch-disp}}^{(20)} + E_{\text{disp}}^{(2)}[\text{CCD}] \\ & + E_{\text{disp}}^{(2)}[\text{S(CCD)}] + E_{\text{disp}}^{(2)}[\text{T(CCD)}], \end{aligned} \quad (17)$$

where $E_{\text{disp}}^{(2)}[\text{CCD}]$ is the two-body CCD dispersion, and $E_{\text{disp}}^{(2)}[\text{S(CCD)}]$ and $E_{\text{disp}}^{(2)}[\text{T(CCD)}]$ are the perturbative corrections due to singles and triples, respectively. Note that CCD dispersion completely replaces all perturbation-theory based SAPT dispersion terms through second order, excepting

$E_{\text{exch-disp}}^{(20)}$. Similarly, we can then write the SAPT2+(3)(CCD) and SAPT2+3(CCD) dispersion energies,

$$E_{\text{disp}}^{\text{SAPT2+3}(CCD)} = E_{\text{disp}}^{\text{SAPT2+}(CCD)} + E_{\text{disp}}^{(30)} \quad (18)$$

$$\begin{aligned} E_{\text{disp}}^{\text{SAPT2+3}(CCD)} = & E_{\text{disp}}^{\text{SAPT2+}(CCD)} + E_{\text{exch-disp}}^{(30)} \\ & + E_{\text{ind-disp}}^{(30)} + E_{\text{exch-ind-disp}}^{(30)}, \end{aligned} \quad (19)$$

where all terms of third order in v are computed purely perturbatively as before.

As a final note, we point out that categorization of SAPT terms can be somewhat nontrivial, even excluding δMP2. For example, we always categorize $E_{\text{exch-ind}}$ terms as induction, though one is equally justified, at least mathematically, to categorize these terms as exchange. We view cross terms involving exchange to be a corrective term to the other components to ensure proper antisymmetry of the underlying wave function. For this same reason we also categorize $E_{\text{exch-disp}}$ terms as dispersion. More ambiguity arises with the $E_{\text{ind-disp}}$ and $E_{\text{exch-ind-disp}}$ terms, both of which we categorize with dispersion interactions. Again, we use chemical rather than mathematical arguments, where we view both terms as corrections to a dispersion interaction based on the orbital deformation computed in induction terms.

3. SAPT Components Summary

For the convenience of the reader, we summarize the terms included in each SAPT component at each level of SAPT considered, in Table I.

B. Databases

In our previous work,³⁴ we analyzed the performance of SAPT total interaction energies using the S22, NBC10, HBC6, and HSG databases for a total of 345 dimers.³⁴ Here we examine a much larger set of 4569 dimers, drawn from several diverse datasets: SSI,⁸⁹ S66x8,^{90,91} HBC6,^{92,93} NBC10ext,^{90,93,94} X31x10,^{58,95} and Ion38,⁹⁶ described in more detail below and in reference 58. For all data, we compute up to SAPT2+3(CCD)δMP2 using jun-cc-pVDZ, aug-cc-pVDZ, and aug-cc-pVTZ basis sets. The jun-cc-pVDZ basis set is the same as aug-cc-pVDZ, but with all diffuse functions on hydrogen and all diffuse *d* functions on heavy atoms removed.⁹⁷ For reference values, we use estimates of the CCSD(T)/CBS limit, with the particular details varying by necessity because they come from multiple sources. All databases used are summarized in Table II.

The sidechain-sidechain interaction (SSI) database contains 3380 interacting amino acid sidechain pairs curated by fragmenting a set of 47 proteins.⁸⁹ The S66x8 dataset is derived from the S66 set of small molecular dimers relevant to biological systems,⁹¹ and includes eight radial displacements between 0.9x and 2.0x the equilibrium intermonomer separation for each dimer for a total of 528 dimers. Monomer geometries

TABLE I. Terms included in each SAPT energy component.

SAPT Level	Elst.	Exch.	Ind.	Disp.
SAPTO	$E_{\text{elst}}^{(10)}$	$E_{\text{exch}}^{(10)}$	$E_{\text{ind,r}}^{(20)} + E_{\text{exch-ind,r}}^{(20)} + \delta E_{\text{HF}}^{[2]}$	$E_{\text{disp}}^{(20)} + E_{\text{exch-disp}}^{(20)}$
sSAPTO	$E_{\text{elst}}^{(10)}$	$E_{\text{exch}}^{(10)}$	$E_{\text{ind,r}}^{(20)} + p_{\text{EX}}(3)E_{\text{exch-ind,r}}^{(20)} + \delta E_{\text{HF}}^{[2]}$	$E_{\text{disp}}^{(20)} + p_{\text{EX}}(3)E_{\text{exch-disp}}^{(20)}$
SAPT2	$E_{\text{elst}}^{(10)} + E_{\text{elst,r}}^{(12)}$	$E_{\text{exch}}^{(10)} + E_{\text{exch}}^{(11)} + E_{\text{exch}}^{(12)}$	$E_{\text{ind,r}}^{(20)} + E_{\text{exch-ind,r}}^{(20)} + \delta E_{\text{HF}}^{[2]}$ + $E_{\text{ind}}^{(22)} + E_{\text{exch-ind}}^{(22)}$	$E_{\text{disp}}^{(20)} + E_{\text{exch-disp}}^{(20)}$
SAPT2+	$E_{\text{elst}}^{(10)} + E_{\text{elst,r}}^{(12)}$	"	"	$E_{\text{disp}}^{(20)} + E_{\text{exch-disp}}^{(20)} + E_{\text{disp}}^{(21)}$ + $E_{\text{disp}}^{(22)}[\text{SDQ}] + E_{\text{disp}}^{(22)[T]}$
SAPT2+(3)	$E_{\text{elst}}^{(10)} + E_{\text{elst,r}}^{(12)} + E_{\text{elst,r}}^{(13)}$	"	"	$E_{\text{SAPT2+}}^{(20)} + E_{\text{disp}}^{(30)}$
SAPT2+3	"	"	$E_{\text{ind,r}}^{(20)} + E_{\text{exch-ind,r}}^{(20)} + E_{\text{ind}}^{(22)}$ + $E_{\text{exch-ind}}^{(22)} + E_{\text{ind,r}}^{(30)} + E_{\text{exch-ind,r}}^{(30)}$ + $\delta E_{\text{HF}}^{[3]}$	$E_{\text{disp}}^{(30)} + E_{\text{exch-disp}}^{(30)}$ + $E_{\text{ind-disp}}^{(30)} + E_{\text{exch-ind-disp}}^{(30)}$
SAPT2+(CCD)	$E_{\text{elst}}^{\text{SAPT2+}}$	"	$E_{\text{ind}}^{\text{SAPT2}}$	$E_{\text{exch-disp}}^{(20)} + E_{\text{disp}}^{(2)}[\text{CCD}]$ + $E_{\text{disp}}^{(2)}[\text{S(CCD)}] + E_{\text{disp}}^{(2)}[\text{T(CCD)}]$
SAPT2+(3)(CCD)	$E_{\text{elst}}^{\text{SAPT2+}(3)}$	"	$E_{\text{ind}}^{\text{SAPT2}}$	$E_{\text{SAPT2+}}^{(30)} + E_{\text{disp}}^{(30)}$
SAPT2+3(CCD)	$E_{\text{elst}}^{\text{SAPT2+3}}$	"	$E_{\text{ind}}^{\text{SAPT2+3}}$	$E_{\text{disp}}^{(30)} + E_{\text{exch-disp}}^{(30)}$ + $E_{\text{ind-disp}}^{(30)} + E_{\text{exch-ind-disp}}^{(30)}$

TABLE II. Datasets used in fitting. All benchmark datasets are of MP2/CBS + ΔCCSD(T)/aug-cc-pVDZ quality or better. For each dataset, we provide the total number of dimers (Size), the number of heavy atoms in the largest dimer (Largest), relevant references, and a brief description. For further details of reference levels of theory for each dataset, please refer to Table SIV in the Supporting Information of Ref. 90.

Database	Size	Largest	Ref.	Description
<i>Potential Curves</i>				
HBC6	118	6	92, 93	dissoc. curves of doubly hydrogen-bonded (HB) complexes
NBC10ext	195	12	93, 94, 90	dissoc. curves of dispersion-bound (DD) complexes
S66×8	528	16	91, 90	dissoc. curves for a balanced mix of biomolecule bonding motifs
X31×10	310	18	95	dissoc. curves of organic halide, halohydride, & halogen complexes
<i>Extracted from Biological Systems</i>				
SSI	3380	20	89	peptide sidechain-sidechain complexes
<i>Charged Small-molecule Dimers</i>				
Ion38	38	8	96, 98	composition of IL16, AHB21 and CHB6
<i>Total</i>	4569	20		

tries are not relaxed along the dissociation.^{90,91} The hydrogen-bonded curve (HBC6) database contains fully relaxed dissociation curves of six unique dimers exhibiting common bidentate hydrogen bonding patterns.^{92,93} Ten dispersion-bound complexes make up the non-bonded curve (NBC10ext) dataset, which includes radial displacements resulting in a total of 195 structures.^{90,93,94} The X31x10 dataset contains 31 dimers composed of halide, halohydride, and halogen complexes, including ten structures along each dissociation coordinate.^{58,95}

To include additional charged dimers in evaluating the levels of SAPT, we add a dataset of 38 ionic dimers which here we name Ion38. This dataset is a composition of three collections of charged dimers used by Lao et al.,^{96,98} specifically the 20 dimers of the anionic hydrogen-bonded set (AHB21), 3 dimers of the cationic hydrogen-bonded dimers set (CHB6), and 15 cation/anion pairs from the IL16 test set. The dimers selected for Ion38 are detailed in the Supplementary Material.

All SAPT computations were run using the Psi4 quantum chemistry software.⁷⁴ Psi4 1.4 was used for nearly all computations, and we do not recommend using versions older than 1.4 due to a fix in third order SAPT induction. We use Psi4 1.5 for computations involving alkali metal cations, as it remedies issues related to the treatment of frozen core orbitals

in the δMP2 correction seen only in these edge cases. All correlated computations employed frozen core orbitals (core molecular orbitals are constrained to remain doubly occupied), and a “dimer centered” basis set is used in the SAPT computations (the union of the basis sets for monomer A and monomer B). Supermolecular computations employed the Boys-Bernardi counterpoise correction.⁹⁹ No midbond functions were employed in the present study.

III. RESULTS

We organize our analysis as follows. First, we re-examine the performance of the levels of SAPT by comparing their total interaction energies to CCSD(T)/CBS benchmarks. We are particularly interested in how the expanded dataset of this work alters any of our previously drawn conclusions from Ref. 34. Following this, we analyze the convergence of the interaction energy components with respect to both level of SAPT and basis set. Finally, based on this analysis we consider a focal-point correction scheme^{68,69} for dispersion to achieve high-quality dispersion energies at a reduced computational cost.

In our analysis, we present mean capped unsigned relative

errors (MCUREs); this is a relative error metric designed to avoid singularities exhibited by small interaction energies.⁹⁰ MCUREs are computed by taking the mean of the capped relative errors (CRE), defined using the computed interaction energy (E_{int}), the reference interaction energy (E_{ref}), and the reference interaction energy at the equilibrium intermolecular distance, ($E_{\text{ref,eq}}$),

$$\text{CRE} = \left(\frac{E_{\text{int}} - E_{\text{ref}}}{E_{\text{weight}}} \right), \quad (20)$$

$$E_{\text{weight}} = \max \left\{ |E_{\text{ref}}|, \frac{\xi |E_{\text{ref}} - E_{\text{ref,eq}}|}{z^3} \right\}, \quad (21)$$

where ξ is a dimensionless parameter controlling the capping strength, set to 0.2 consistent with Refs. 90 and 100. The quantity z is the ratio between the dimer's intermolecular distance and the corresponding equilibrium distance. For SSI and Ion38, which do not contain dimers on displacement curves, we use a capping value of 0.5 kcal mol⁻¹, consistent with Ref. 90.

A. Analysis of Total Interaction Energies

1. jun-cc-pVDZ and aug-cc-pVDZ

In Figure 1, we present mean absolute errors (MAEs), MCUREs, and the distributions of total interaction energy errors for the levels of SAPT considered, using our complete set of molecular dimers. The Figure presents results for the jun-cc-pVDZ, aug-cc-pVDZ, and aug-cc-pVTZ basis sets, as well as a set of results denoted aug-cc-pV[DT]Z using the aug-cc-pVTZ basis for Hartree–Fock dependent terms, and a two-point basis set extrapolation¹⁰¹ using the aug-cc-pVDZ and aug-cc-pVTZ basis sets for the electron-correlation dependent terms. For comparison, results from supermolecular MP2 are also provided in the leftmost column. In this section, we will focus on the jun-cc-pVDZ and aug-cc-pVDZ results, and aug-cc-pVTZ results and extrapolated results are discussed below.

Although we present the complete set of data, we note at the outset that it is not generally advisable to use highly correlated methods like SAPT2+3(CCD), etc., with modest basis sets like jun-cc-pVDZ and aug-cc-pVDZ. In wavefunction-based quantum chemistry, terms depending on electron correlation need larger basis sets like aug-cc-pVTZ for good performance. In alignment with this expectation, increasing the order of the perturbative treatment does not lead to lower errors using the jun-cc-pVDZ basis set, due to the limited size of the basis set. For the slightly larger aug-cc-pVDZ basis, which improves upon jun-cc-pVDZ by adding diffuse functions to hydrogen atoms and diffuse d functions to heavy atoms, there are some significant improvements in error statistics upon going to the higher levels of SAPT beyond SAPT0, although there is no advantage on average in going beyond SAPT2+3.

Noticeable for both basis sets, the inclusion of the $\delta\text{MP}2$ correction causes all methods to produce systematically underbound interaction energies, with errors larger than the underlying uncorrected SAPT methods. Similarly, for these ba-

sis sets improving the correlation treatment by using CCD amplitudes for dispersion terms also degrades performance of overall total interaction energies, though not in such a way as to cause systematic over- or underbinding relative to corresponding levels of SAPT without CCD dispersion.

For these small basis sets, the optimal performance for total interaction energies results from a cancellation of errors between basis set effects and an approximate treatment of electron correlation. When using the jun-cc-pVDZ basis set, SAPT0 exhibits the lowest MAE and MCURE, despite being the least computationally expensive method. Improving the basis set to aug-cc-pVDZ improves the error statistics for SAPT0.

When using aug-cc-pVDZ, SAPT2+3 produces the lowest MAEs, while SAPT2+ shows the lowest relative error. These statistics, along with the distributions of absolute errors, are similar between SAPT2+ and SAPT2+3 despite the fairly significant difference in their computational costs. In fact, the remarkably small MAE of 0.18 kcal mol⁻¹, the low relative error of around 7%, and the even distribution of absolute errors make SAPT2+/aug-cc-pVDZ comparable to much more expensive variants of SAPT in larger basis sets, as shown in more detail below, at least for total interaction energies. Our previous designation of SAPT2+/aug-cc-pVDZ as the “silver” level of SAPT is thus confirmed when considering the larger dataset presented here.

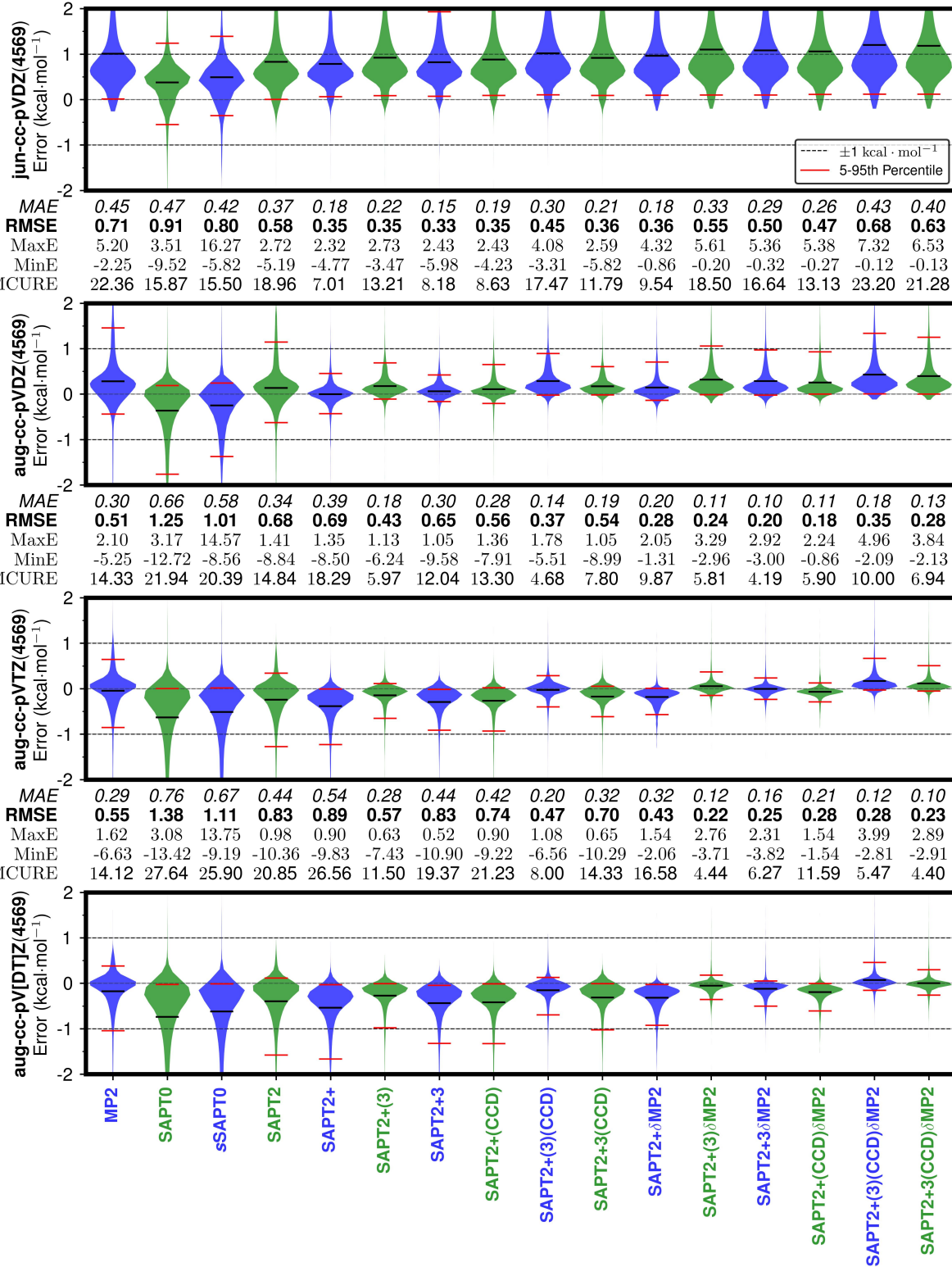
Based on the larger dataset of the present study, our earlier recommendation³⁴ of *s*SAPT0/jun-cc-pVDZ as the “bronze” level needs to be updated. From Figure 1, clearly *s*SAPT0/jun-cc-pVDZ is slightly worse than SAPT0/jun-cc-pVDZ, and both levels of theory are significantly worse in comparison to the corresponding aug-cc-pVDZ values, particularly with respect to MCURE. For both basis sets, the scaling done in *s*SAPT0 has little effect on the MAE and MCURE vs SAPT0, while producing some highly underbound outliers. To understand the discrepancy between our previous conclusions and the data in Figure 1, we show plots of MAEs and MCUREs for each individual data set in Figure 2. From this data, *s*SAPT0 only outperforms SAPT0 for HBC6, and the effect of the scaling is effectively negligible for all other datasets. Empirically, we have found scaling in SAPT0 to improve performance of total interaction energies for strongly hydrogen-bound complexes.⁸⁰ We note that the scaling factor in *s*SAPT0 was chosen as to minimize errors between *s*SAPT0/jun-cc-pVDZ and CCSD(T)/CBS for the HBC6 dataset. Therefore, this improvement for HBC6 can be perhaps viewed as intentional overfitting, though this scaling does not seem to degrade performance in the other datasets.

Interestingly, SAPT0 and *s*SAPT0 perform much worse for the SSI database when using jun-cc-pVDZ over aug-cc-pVDZ, nearly by a factor of two for both methods. The opposite trend is seen in NBC10ext, where jun-cc-pVDZ results in much better total interaction energies. SAPT0 MCURE statistics benefit greatly from the larger basis set when applied to X31x10. The larger aug-cc-pVDZ basis set is better for Ion38, but worse for HBC6, compared to jun-cc-pVDZ.

SSI contains mostly weakly-bound amino acid sidechain

FIG. 1. Mean absolute errors, root mean square errors, minimum and maximum errors (kcal mol⁻¹), MCUREs (%), and distributions of errors via violin plots for selected levels of SAPT with respect to CCSD(T)/CBS best estimates. Interaction energies are computed for the SSI, S66x8, HBC6, NBC10ext, X31x10, and Ion38 databases for a total of 4569 dimer geometries.

<i>MAE</i>	1.01	0.57	0.59	0.85	0.80	0.93	0.84	0.89	1.02	0.93	0.96	1.10	1.08	1.06	1.20	1.18
<i>RMSE</i>	1.39	0.83	0.96	1.11	0.98	1.13	1.00	1.10	1.25	1.12	1.23	1.41	1.39	1.36	1.54	1.52
MaxE	7.75	6.25	19.17	5.73	4.77	5.88	5.28	6.57	7.98	5.52	8.03	9.44	8.98	10.12	11.53	10.99
MinE	-0.26	-8.36	-4.63	-4.11	-3.67	-3.11	-4.99	-3.69	-3.13	-5.00	-0.25	-0.20	-0.20	-0.24	-0.20	-0.20
MCURE	56.63	40.11	41.43	49.84	49.63	56.89	52.18	54.12	61.40	56.67	56.63	63.94	62.94	61.15	68.46	67.46



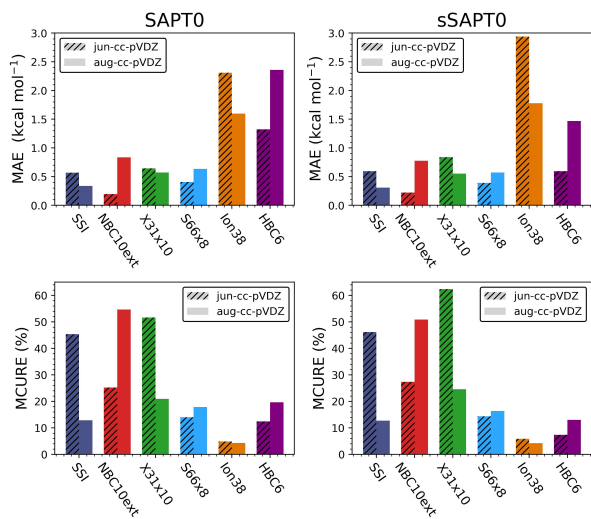


FIG. 2. Total interaction energy MAEs (kcal mol^{-1}) and MCURE(%) of all six datasets, computed using SAPTO and sSAPTO with jun-cc-pVDZ and aug-cc-pVDZ basis sets. Bars plotted with hash marks represent data computed using jun-cc-pVDZ, and bars without hash marks correspond to aug-cc-pVDZ.

monomers, with interaction energies typically significantly smaller than those found in HBC6 or NBC10ext. SSI interactions can be electrostatics-dominated, dispersion-dominated, or have a mixed influence, depending on the sidechain. In Figure 3, we plot the interaction energy errors of SSI computed using SAPTO/jun-cc-pVDZ and SAPTO/aug-cc-pVDZ, where the errors are plotted on a grid organized by the amino acid involved in the dimer. SAPTO/jun-cc-pVDZ tends to underbind all interaction types, and is the most accurate for interactions between two aromatic residues or two nonpolar residues. SAPTO/aug-cc-pVDZ only slightly underbinds interactions between two aliphatic nonpolar residues, while tending to overbind all other interaction pairs. These plots also show SAPTO/jun-cc-pVDZ performing better for dispersion-dominated complexes in comparison to SAPTO/aug-cc-pVDZ, consistent with the lower errors seen in NBC10ext with SAPTO/jun-cc-pVDZ compared to SAPTO/aug-cc-pVDZ. The formulation of dispersion in SAPTO closely resembles MP2, which is well-known to overbind π - π complexes in general, although it can produce reasonable results when combined with a relatively small basis set.¹² Later in this work, we will show that this compensation of errors is not solely due to dispersion, but to an improved cancellation of errors between exchange and dispersion in jun-cc-pVDZ compared to aug-cc-pVDZ.

Looking at both summative statistics and individual data subsets, the optimal low-cost SAPT variant seems to be somewhat context dependent. Firstly, adoption of the scaling in sSAPTO has a relatively negligible effect on the average accuracy of total interaction energies outside its application to the HBC6 dataset, where it is quite helpful. While this choice does not seem to significantly degrade average performance of sSAPTO when applied to the other datasets, we do see it

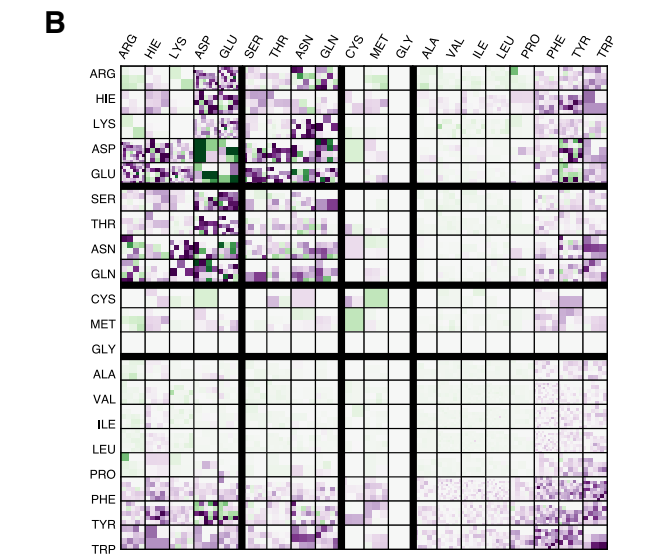
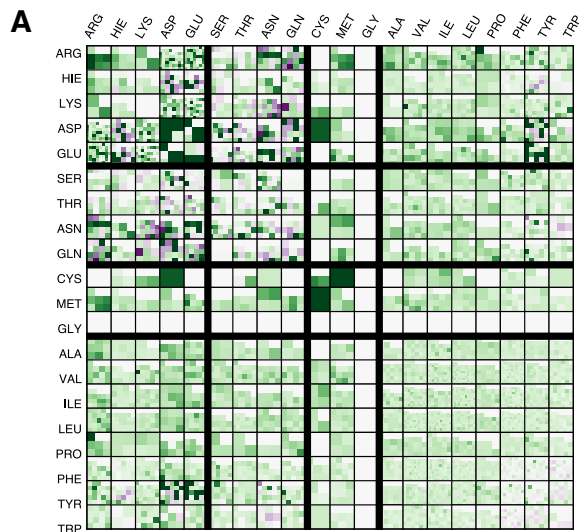


FIG. 3. Total interaction energy errors of the SSI dataset computed with (a) SAPTO/jun-cc-pVDZ and (b) SAPTO/aug-cc-pVDZ. Each square represents interaction energy errors for dimers containing the residues corresponding to the given row and column. The colors are saturated at $\pm 1.0 \text{ kcal mol}^{-1}$, with white reflecting no error, green representing underbinding, and purple representing overbinding.

cause a systematic bias towards underbound/overly-repulsive interaction energies in addition to some very largely underbound outliers. Therefore, sSAPTO/aug-cc-pVDZ is only recommended when applied to very close contacts, particularly of hydrogen-bound systems, where this bias is found to be helpful. Among the least computationally expensive methods, this leaves a choice between SAPTO/jun-cc-pVDZ or SAPTO/aug-cc-pVDZ. While our summative statistics suggest that SAPTO/aug-cc-pVDZ outperforms SAPTO/jun-cc-pVDZ on average, certain relevant cases including strong hydrogen bonds and dispersion-dominated interactions can be more accurately described by SAPTO/jun-cc-pVDZ. However, based on performance using the large SSI database, SAPTO ben-

efits greatly from the larger aug-cc-pVDZ basis set, suggesting that SAPT0/aug-cc-pVDZ is the preferred low-cost (“bronze”) SAPT method for treating interactions involving proteins and potentially other biologically relevant systems.

2. aug-cc-pVTZ and aug-cc-pV[DT]Z

We report total interaction energy errors for all levels of SAPT discussed here using aug-cc-pVTZ in Figure 1, where they can be compared to jun-cc-pVDZ and aug-cc-pVDZ results for the full dataset. We also report results of two-point extrapolation¹⁰¹ of SAPT terms depending on electron correlation (and using aug-cc-pVTZ for remaining terms), denoted aug-cc-pV[DT]Z.

In contrast to the double- ζ results in Figure 1, in the aug-cc-pVTZ basis, the higher levels of SAPT start to show more of a clear benefit over the lower levels of SAPT. Nevertheless, increasing the perturbation order does not smoothly lead to decreased average errors or tighter error distributions (a general conclusion from our previous study on a smaller test set).³⁴ Among SAPT0, SAPT2+, SAPT2+(3), and SAPT2+3, all methods now improve over SAPT0, but SAPT2 and SAPT2+ show similar error statistics, and SAPT2+(3) performs better than SAPT2+3. All of these methods consistently overbind compared to reference CCSD(T)/CBS results. This may be a consequence of the Rayleigh-Schrödinger corrections being developed at a higher level than the exchange ones. For example, SAPT2+ performs worse on average than SAPT2 in an aug-cc-pVTZ basis, perhaps because the additional higher-order dispersion terms are not damped by corresponding exchange terms. Adding CCD dispersion improves SAPT2+, SAPT2+(3), and SAPT2+3, but SAPT2+(3)(CCD) remains better than SAPT2+3(CCD). CCD dispersion mitigates the systematic overbinding of SAPT2+ through SAPT2+3, and the mean error of SAPT2+(3)(CCD) is very close to zero.

In the aug-cc-pVTZ basis, the inclusion of the δ MP2 correction significantly improves error statistics, more so than CCD dispersion. Including δ MP2 tends to shift mean errors towards higher values (correcting systematic overbinding in most cases), and error distributions are greatly tightened. This may be because the δ MP2 correction is picking up some higher-order exchange effects that are still not captured at any of the levels of SAPT considered here. Adding δ MP2 corrections substantially improves SAPT2+, SAPT2+(3), and SAPT2+3, and finally SAPT2+3 δ MP2 becomes better on average than SAPT2+(3) δ MP2. Further adding CCD dispersion on top of δ MP2 corrections is beneficial for SAPT2+ δ MP2 but not for SAPT2+(3) δ MP2 or SAPT2+3 δ MP2. Among the aug-cc-pVTZ results, SAPT2+(3) δ MP2, SAPT2+3 δ MP2, and SAPT2+(CCD) δ MP2 perform very well, with similar error statistics. SAPT2+3(CCD) δ MP2 is nearly as good (with slightly larger MAE, RMSE, and MCURE values, and a shift in mean errors slightly towards underbound). SAPT2+(3)(CCD) and SAPT2+(3) also perform quite well in this basis. All of these SAPT methods perform better than supermolecular MP2 in this basis.

Compared to aug-cc-pVDZ, the larger aug-cc-pVTZ ba-

sis improves error statistics for all methods employing the δ MP2 correction, except for SAPT2+ δ MP2, which performs about the same in both basis sets; this is consistent with the reduction in errors in supermolecular MP2 for this basis set improvement. The larger basis also significantly reduces errors for SAPT2+(3)(CCD). For other methods, there is a similar performance in both basis sets [SAPT2, SAPT2+(3), SAPT2+3(CCD)], or the results actually get worse, presumably from a less favorable cancellation of method and basis set errors. For SAPT0, SAPT2, SAPT2+, SAPT2+3, SAPT2+(CCD), and SAPT2+ δ MP2, the error statistics for the total interaction energies show no benefit for improving the basis from aug-cc-pVDZ to aug-cc-pVTZ.

Finally, we may ask if further basis set improvements from aug-cc-pVTZ to aug-cc-pV[DT]Z extrapolated values is beneficial for some of the levels of SAPT. For most of the methods considered, this actually increases errors. The only methods for which a clear improvement in error statistics is seen are the highest levels of SAPT considered, SAPT2+(3)(CCD) δ MP2 and SAPT2+3(CCD) δ MP2. This may be a reflection of the more complete methods having larger basis set requirements due to more complete inclusion of electron correlation effects (which can be highly basis set dependent). The performance of SAPT2+(3) δ MP2 is about the same for aug-cc-pVTZ or aug-cc-pV[DT]Z.

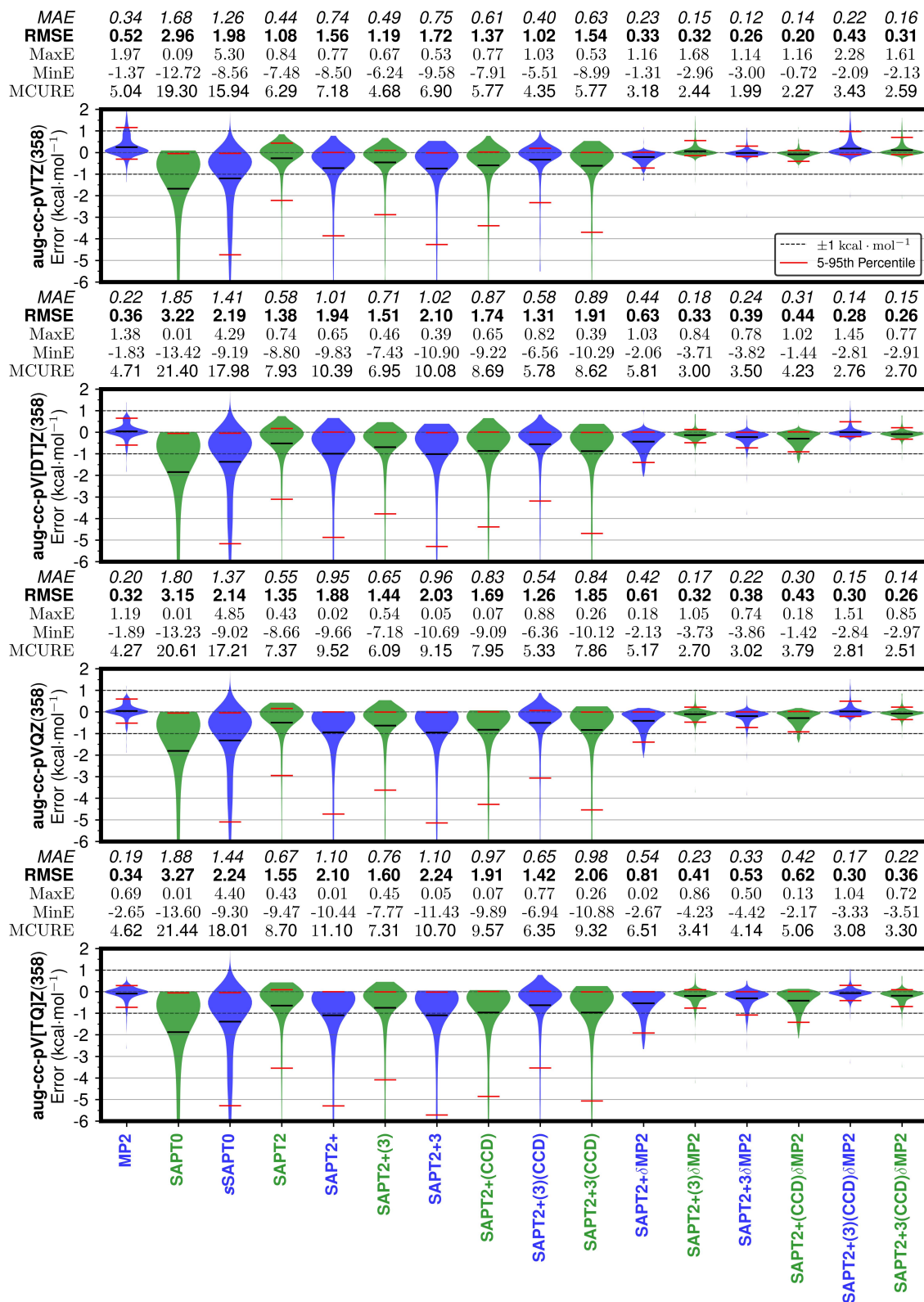
3. aug-cc-pVQZ

We report total interaction energy errors for the aug-cc-pVQZ basis set in Figure 4. This Figure provides results for a subset of 358 dimers from our full dataset, to make the computations more tractable. For comparison purposes, for this same 358-dimer subset, the Figure also contains results for the aug-cc-pVTZ basis, and aug-cc-pV[DT]Z and aug-cc-pV[TQ]Z extrapolated results.

The error statistics for MP2 itself are quite favorable for this 358-dimer subset, and MP2 outperforms all but the best SAPT levels considered. This is not the case for the full subset data presented in Figure 1. This is likely due to the subset having a heavy representation of strongly interacting, electrostatically dominated dimers: 118 geometries are for doubly hydrogen bonded dimers from the HBC6 database, and 24 are from the Ion38 subset; the remaining 216 are taken from the S66x8 subset of mixed interaction types.

For the subset, increasing the basis set treatment from aug-cc-pVTZ to aug-cc-pV[DT]Z extrapolated values does not improve SAPT error statistics except for the two highest levels of SAPT, SAPT2+(3)(CCD) δ MP2 and SAPT2+3(CCD) δ MP2. This is consistent with our findings for the complete 4569-dimer test set. Error statistics for the aug-cc-pV[DT]Z extrapolation are remarkably similar to the aug-cc-pVQZ error statistics, suggesting that the DT extrapolation provides an excellent approximation to aug-cc-pVQZ results. Due to the unfavorable scaling of the computational cost with the number of basis functions ($o^3 v^4$ for the $E_{\text{disp}}^{(22)}$ term, where o and v are the number of occupied and virtual orbitals, respectively), this

FIG. 4. Mean absolute errors, root mean square errors, minimum and maximum errors (kcal mol^{-1}), MCUREs (%), and distributions of errors via violin plots of selected levels of SAPT with respect to CCSD(T)/CBS best estimates. Due to the cost of using the aug-cc-pVQZ basis set with higher-order SAPT methods, only a subset of 358 dimers from the HBC6, Ion38, and a subset of the S66x8 datasets are displayed for aug-cc-pVTZ, aug-cc-pV[DT]Z, aug-cc-pVQZ and aug-cc-pV[TQ]Z.



indicates that DT basis set extrapolation is an excellent alternative to much more costly aug-cc-pVQZ computations.

On the other hand, just like the aug-cc-pV[DT]Z extrapolations, the aug-cc-pVQZ values are not improved over aug-cc-pVTZ except for the two highest SAPT levels considered, SAPT2+(3)(CCD) δ MP2 and SAPT2+3(CCD) δ MP2. The MAE, RMSE, and MCURE for SAPT2+(3)(CCD) δ MP2 are excellent, at 0.15 and 0.30 kcal mol⁻¹, and 2.8% in the aug-cc-pVQZ basis, and these improve very slightly to 0.14 and 0.26 kcal mol⁻¹, and 2.5% for SAPT2+3(CCD) δ MP2. The estimates from DT basis set extrapolation are extremely similar.

For all other levels, it seems best to stop at aug-cc-pVTZ (or earlier at aug-cc-pVDZ, for methods discussed in the previous subsection). If we attempt to improve the basis set further by extrapolating aug-cc-pVTZ and aug-cc-pVQZ results, the error statistics get worse for all methods considered. This suggests that further improvements in error statistics would require additional higher-order SAPT terms. In fact, by favorable cancellation of errors, two SAPT levels with the aug-cc-pVTZ basis exhibit even better error statistics than SAPT2+(3)(CCD) δ MP2 and SAPT2+3(CCD) δ MP2 in the larger aug-cc-pVQZ basis. The MAE, RMSE, and MCURE for SAPT2+3 δ MP2/aug-cc-pVTZ are 0.12 and 0.26 kcal mol⁻¹, and 2.0%, and for SAPT2+(CCD) δ MP2/aug-cc-pVTZ they are 0.14 and 0.20 kcal mol⁻¹ and 2.3%.

4. Most Accurate Levels of Theory for Total Interaction Energies

The results for the 358-dimer subset in Figure 4 indicate that the aug-cc-pV[DT]Z extrapolated results have nearly the same error statistics as explicit aug-cc-pVQZ results. They further indicate that basis sets beyond aug-cc-pVQZ are not beneficial for these levels of SAPT. The most accurate methods for the subset were SAPT2+3 δ MP2 and SAPT2+(CCD) δ MP2 in the aug-cc-pVTZ basis, and SAPT2+(3)(CCD) δ MP2 and SAPT2+3(CCD) δ MP2 in the aug-cc-pVQZ basis or using aug-cc-pV[DT]Z extrapolations.

These findings for the subset are consistent with the findings for the full dataset, where the lowest errors are seen for SAPT2+3 δ MP2 and SAPT2+(CCD) δ MP2 in the aug-cc-pVTZ basis, or with SAPT2+(3)(CCD) δ MP2 and SAPT2+3(CCD) δ MP2 using aug-cc-pV[DT]Z extrapolation. Error statistics for all of these methods are quite similar (MAE 0.10-0.12 kcal mol⁻¹, RMSE 0.18 to 0.28 kcal mol⁻¹, MCURE 4.2-5.9%, with SAPT2+3 δ MP2/aug-cc-pVTZ and SAPT2+(CCD) δ MP2/aug-cc-pVTZ having the lower RMSE's). In addition, SAPT2+(3) δ MP2 features very similar error statistics for the full dataset, using either an aug-cc-pVTZ basis or aug-cc-pV[DT]Z extrapolation. From a practical point of view, SAPT2+(3) δ MP2/aug-cc-pVTZ is the least computationally expensive method among these, with error statistics that are nearly as good. Thus, we confirm the earlier conclusion³⁴ based on a much smaller dataset, that SAPT2+(3) δ MP2/aug-cc-pVTZ is a good choice for a “gold” standard of SAPT.

Previously, we recommended³⁴ SAPT2+(CCD) δ MP2 as a “platinum” standard when the most accurate results are desired, regardless of computational cost. In the present study, we see that the error statistics are not any better than those of the “gold” standard method, SAPT2+(3) δ MP2, except for a very small reduction in the RMSE. On the other hand, in this study we were able to examine the effect of larger basis sets beyond aug-cc-pVTZ on the most complete SAPT methods, and we see that aug-cc-pV[DT]Z basis set extrapolation, or use of the larger aug-cc-pVQZ basis, improves results for the highest-level SAPT methods, SAPT2+(3)(CCD) δ MP2 and SAPT2+3(CCD) δ MP2, making them competitive with “gold” standard SAPT2+(3) δ MP2/aug-cc-pVTZ. Indeed, SAPT2+3(CCD) δ MP2/aug-cc-pV[DT]Z has very slightly improved error statistics, in every category, compared to SAPT2+(3) δ MP2/aug-cc-pVTZ, suggesting that if a “platinum” standard is desired, then this would be it. However, the improvement over the “gold” level is very tiny indeed, and the increase in computational cost is dramatic due to the use of CCD dispersion.

B. Analysis of Interaction Energy Components

Thus far, our analysis has centered on the ability of SAPT to accurately compute total interaction energies. One of the hallmark features of SAPT is its ability to provide additional insight into the nature of noncovalent interactions by means of interaction energy components. Here, we analyze the behavior of these components with respect to basis set and SAPT method.

1. Basis Set Convergence of SAPT Components

Figure 5 displays basis set errors for all levels and all components of SAPT computed with the aug-cc-pVDZ and aug-cc-pVTZ basis sets. Results are shown for our 358-dimer subset described above (using HBC6, Ion38, and a subset of S66x8). Here, basis set error is defined as the error between a given total or component interaction energy and its value in the aug-cc-pVQZ basis. Mean absolute basis set errors for aug-cc-pVDZ are plotted with dashed lines, and solid lines for aug-cc-pVTZ. Note that we label the x-axis using the level of SAPT, and that many levels of SAPT share the same component definitions (see Table I).

Except for the dispersion component (and total interaction energy), SAPT0 and sSAPT0 show only a small basis set dependence. This is because all (s)SAPT0 components except dispersion are captured at the Hartree–Fock level, and HF converges much faster with respect to basis set than energies depending on electron correlation.

Figure 5 shows basis set errors for electrostatics in red. This component converges to its basis set limit rather quickly across all methods. $E_{\text{elst}}^{(10)}$, which makes up the entirety of the electrostatic component in SAPT0, shows agreement between aug-cc-pVDZ, aug-cc-pVTZ, and aug-cc-pVQZ to

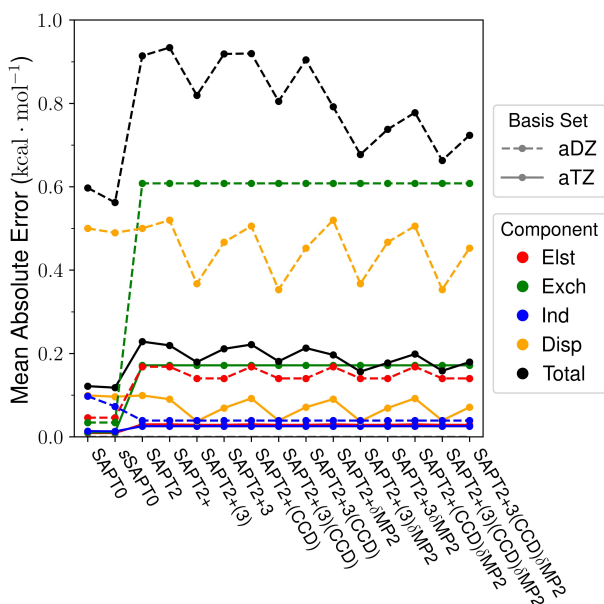


FIG. 5. Mean absolute basis set errors (kcal mol^{-1}) of SAPT total and component energies. Basis set errors are computed as the difference in SAPT total or component interaction energy computed using aug-cc-pVDZ (dashed lines) or aug-cc-pVTZ (solid lines), with respect to the same SAPT level using aug-cc-pVQZ. All data are computed with the small subset (358 dimers) of our complete database described in the text.

within about $0.05 \text{ kcal mol}^{-1}$ MAE. Electron correlation dependent terms $E_{\text{elst,r}}^{(12)}$ and $E_{\text{elst,r}}^{(13)}$ show larger MAE at aug-cc-pVDZ ($\sim 0.2 \text{ kcal mol}^{-1}$), though the basis set errors are negligible when aug-cc-pVTZ is used. The aug-cc-pVTZ and aug-cc-pVQZ electrostatics are in such good agreement that the former basis set is sufficient for benchmarking electrostatic interactions.

Exchange-repulsion, shown in green, converges more slowly with respect to basis set than does electrostatics, and it is almost always the component with the largest basis set errors for SAPT levels beyond SAFT0 (around 0.6 and $0.2 \text{ kcal mol}^{-1}$ MAE for aug-cc-pVDZ and aug-cc-pVTZ, respectively). Thus, $E_{\text{exch}}^{(11)} + E_{\text{exch}}^{(12)}$, the correlation-dependent exchange corrections in all levels of SAPT beyond SAFT0, are slowly convergent with respect to basis.

Induction, shown in blue, shows very small MAE due to basis set, even for aug-cc-pVDZ. Because we always include δE_{HF} in this work, our levels of SAPT include only three distinct levels for induction: SAFT0, sSAFT0, and SAFT2 and beyond (see Table I). The induction basis set mean absolute errors are negligible except for SAFT0 and sSAFT0, where the MAE is closer to $0.1 \text{ kcal mol}^{-1}$ in the aug-cc-pVDZ basis set (and negligible for aug-cc-pVTZ). Induction terms are added in pairs, specifically a E_{ind} term and a $E_{\text{exch-ind}}$ term; these two terms are always opposite in magnitude. Below, we analyze some specific cases in which most of the induction terms are very insensitive to basis set, while the third-order induction terms $E_{\text{ind}}^{(30)}$ and $E_{\text{exch-ind}}^{(30)}$ are somewhat sensitive to

basis. However, the basis set errors in those two terms tend to be very similar, but with opposite signs, making the overall induction contribution rather insensitive to basis.

Like exchange, dispersion shows more pronounced basis set dependence in comparison to electrostatics and induction. By increasing the basis set from aug-cc-pVDZ to aug-cc-pVTZ, the basis set MAE in dispersion decreases from around $0.5 \text{ kcal mol}^{-1}$ to approximately $0.1 \text{ kcal mol}^{-1}$. Use of CCD dispersion instead of perturbative dispersion has no noticeable effect on the basis set errors for either basis set. Similar to induction, dispersion contains cross-terms at each intermolecular perturbation order, e.g. $E_{\text{exch-disp}}^{(20)}$ is included for second-order dispersion. SAPT2+(3), however, only includes $E_{\text{disp}}^{(30)}$ as a third order term and ignores all other third-order cross terms, which are included in SAPT2+3. A surprising byproduct of this partial third order dispersion is that a reduced basis set error is observed.

For further detail into the basis set convergence of SAPT components, we plot all SAPT components computed using aug-cc-pVDZ, aug-cc-pVTZ, and aug-cc-pVQZ basis sets for the water dimer along its dissociation coordinate in Figure 6. For clarity, we plot the CCD dispersion terms separately from the purely perturbative ones. Even for a dimer like this with an interaction energy dominated by electrostatics, each electrostatic term shows no significant difference between basis sets. This result is consistent with the basis set insensitivity of $E_{\text{elst}}^{(10)}$; in this case, the correlation-dependent terms are both very small. For exchange-repulsion, the agreement is excellent among all three basis sets for $E_{\text{exch}}^{(10)}$ and $E_{\text{exch}}^{(11)}$. Conversely, $E_{\text{exch}}^{(12)}$ does show some significant basis set dependence at short range. Here, aug-cc-pVDZ predicts the value of $E_{\text{exch}}^{(12)}$ to be too large, causing the cumulative exchange-repulsion component to be about $0.5 \text{ kcal mol}^{-1}$ too positive at equilibrium. This overly-repulsive term is mostly corrected when using aug-cc-pVTZ. Thus, SAPT electrostatics seem to be converged to within quantitative accuracy even with aug-cc-pVDZ, while exchange requires aug-cc-pVTZ for similar agreement.

In Fig. 6, $E_{\text{ind,r}}^{(20)}$ and $E_{\text{exch-ind,r}}^{(20)}$ are of similar magnitude and fairly large (as is typical), and the values computed with all three basis sets agree remarkably well. Increasing intramolecular perturbation with $E_{\text{ind}}^{(22)}$ and $E_{\text{exch-ind}}^{(22)}$ produces smaller-magnitude terms, and they also show extremely close agreement among the three basis sets studied. Induction terms of third-order in intermolecular perturbation are even larger than the corresponding second order terms. Furthermore, a significant basis set dependence is observed as well, where terms computed with aug-cc-pVDZ are too small in magnitude by about 1 kcal mol^{-1} in comparison to those computed with aug-cc-pVTZ and aug-cc-pVQZ, which show very close agreement. When $E_{\text{ind,r}}^{(30)}$ and $E_{\text{exch-ind,r}}^{(30)}$ are summed, these basis set errors cancel very well such that the agreement among the three basis sets is within $0.1 \text{ kcal mol}^{-1}$. We also categorize the supermolecular δE_{HF} correction terms as induction. As expected, for both $\delta E_{\text{HF}}^{[2]}$ and $\delta E_{\text{HF}}^{[3]}$, we observe very close agreement among the three basis sets used.

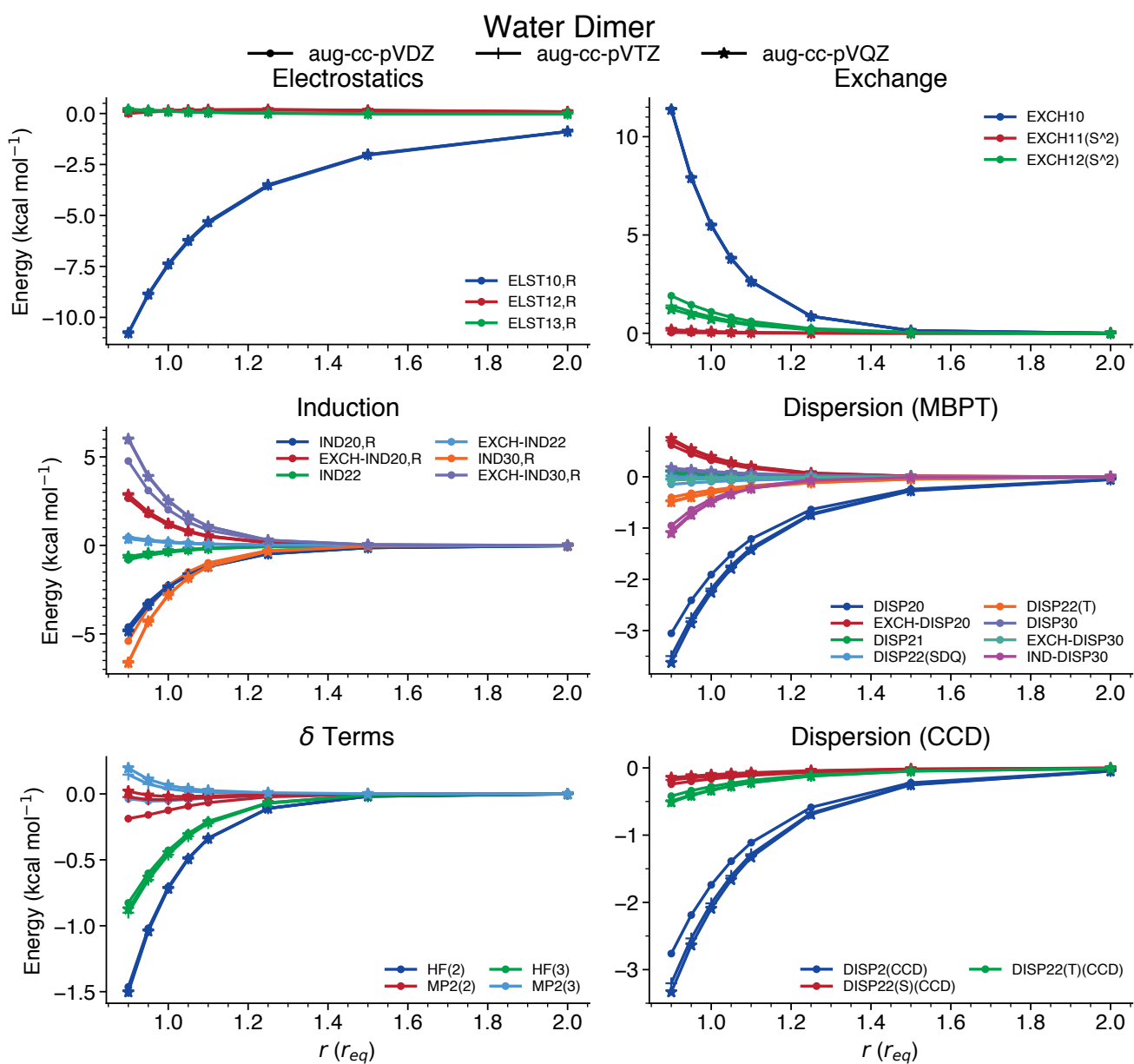


FIG. 6. Absolute interaction energy components of the water dimer. We plot all SAPT components for the water dimer as a function of inter-monomer separation in units of equilibrium distance (r_{eq}), computed using aug-cc-pVDZ, aug-cc-pVTZ, and aug-cc-pVQZ basis sets.

For dispersion, the largest-magnitude terms are $E_{\text{disp}}^{(20)}$ and $E_{\text{exch-disp}}^{(20)}$, i.e., the ones captured by SAPTO. These terms show good agreement between aug-cc-pVTZ and aug-cc-pVQZ, and aug-cc-pVDZ produces values that are in general too small in magnitude, by up to about 0.5 kcal mol⁻¹ at short range for $E_{\text{disp}}^{(20)}$. The same trend is seen with the three CCD terms, though the difference between aug-cc-pVTZ and aug-cc-pVQZ is slightly more pronounced. While we saw cancellation of errors with the third order induction terms, here the difference between aug-cc-pVDZ and aug-cc-pVQZ is much smaller for $E_{\text{exch-disp}}^{(20)}$ than it is for $E_{\text{disp}}^{(20)}$, causing the disper-

sion component to be underbound when aug-cc-pVDZ is used. Since this effect occurs in the second order terms, this underbinding is potentially expected at all levels of SAPT and thus only curable with either an increased basis set or some type of basis set correction. Third order dispersion terms are comparatively much less sensitive to basis set than the second order terms. $E_{\text{exch-disp}}^{(30)}$ and $E_{\text{disp}}^{(30)}$ have cancelling errors, while $E_{\text{ind-disp}}^{(30)}$ has a small difference between aug-cc-pVDZ and aug-cc-pVQZ only noticeable at very short range.

Finally, the basis set errors of $\delta E_{\text{MP2}}^{[2]}$ and $\delta E_{\text{MP2}}^{[3]}$ are much more prominent. In fact, both δMP2 corrections computed

with aug-cc-pVDZ show qualitatively incorrect behavior with respect to intermolecular separation, and substantial negative errors, compared to the aug-cc-pVQZ results. These observations are consistent with the systematic overbinding of all SAPT methods when using a δ MP2 correction in an aug-cc-pVDZ basis set (see Figure 1). Correct behavior and very small errors are restored by the time aug-cc-pVTZ is used.

The Supplementary Material contains additional Figures of the SAPT energy terms plotted against intermolecular separation distance for other members of the S66x8 test set. The results for water dimer discussed in this section are typical.

2. Convergence of SAPT Components with Level of Theory

We have shown that all but a few SAPT terms converge very quickly with respect to basis set; in some cases even aug-cc-pVDZ is sufficient for quantitative accuracy (especially for the Hartree–Fock dependent terms). Next, we will discuss how the accuracy of each component converges with respect to increasing level of SAPT. Unlike for total interaction energies, where high-level benchmark protocols are established, component energies have no easily accessible exact or near-exact solution.

In Figure 7, we present MAEs, MCUREs, and error distributions for all SAPT components computed with jun-cc-pVDZ, aug-cc-pVDZ, and aug-cc-pVTZ. SAPT2+3(CCD)/aug-cc-pVTZ is used as our reference level of theory, as it performs well for total interaction energies and it is in principle the most complete method considered here except for the lack of a δ E_{MP2} correction, which is not readily assigned to one of the four energy components. In the Figure, components corresponding to the reference level of theory are shown with no error distribution.

Figure 7 shows rather similar error distributions for electrostatics, exchange, and induction as one progresses down rows from jun-cc-pVDZ to aug-cc-pVDZ and then aug-cc-pVTZ. The SAPT0 electrostatics and exchange error distributions are very insensitive to basis, while SAPT0 induction improves somewhat for each basis set improvement. Electrostatics, exchange, and induction computed with the higher levels of SAPT (including electron correlation dependent terms) have error distributions that are somewhat more sensitive to basis. The error distributions in the dispersion terms are by far the most basis set dependent.

Across all levels of theory, the electrostatics terms benefit only slightly from the larger aug-cc-pVDZ basis set in comparison to jun-cc-pVDZ. For both basis sets, the effect of E_{elst,r}⁽¹²⁾ (included in SAPT2 and SAPT2+) is effectively negligible in the MAE, although the RMSE decreases vs SAPT0. However, further inclusion of E_{elst,r}⁽¹³⁾ [in SAPT2+(3) and SAPT2+3] improves most error statistics by around a factor of two. Error distributions for SAPT0 electrostatics for both jun-cc-pVDZ and aug-cc-pVDZ are reasonably balanced, and increasing the level of theory causes these distributions to tighten. In the aug-cc-pVTZ basis, SAPT2 and SAPT2+ offer more of an improvement over SAPT0 than they

did in the double- ζ basis sets.

SAPT0 and sSAPT0 show essentially the same errors for exchange-repulsion when using the jun-cc-pVDZ or aug-cc-pVDZ basis sets, with MAEs over 0.5 kcal mol⁻¹ and strongly underbound error distributions. Adding E_{exch}⁽¹¹⁾ and E_{exch}⁽¹²⁾ (at SAPT2 and beyond) greatly reduces errors. The large, biased errors in SAPT0 exchange-repulsion show small relative errors (about 8%) due to the typically large magnitude of exchange interactions. Nonetheless, for SAPT0/aug-cc-pVDZ, exchange repulsion is likely to be the component with the largest error (as in Fig. 5).

The sSAPT0 induction energies are less accurate than those of conventional SAPT0, again suggesting that SAPT0 is a typically more reliable method. Across each row, the improvement in induction energies from SAPT0 to SAPT2 and beyond is around 0.2 kcal mol⁻¹ in mean absolute error, around the same MAE improvement seen in going from SAPT0 to SAPT2+(3) and beyond for electrostatics (but less than the 0.4 kcal mol⁻¹ or greater improvement in exchange in going from SAPT0 to SAPT2 and beyond). Improvements from SAPT0 to the higher levels of SAPT are somewhat larger in the aug-cc-pVTZ basis sets than for the smaller basis sets (especially for exchange), due to the larger basis set sensitivity of the correlation-dependent terms.

For all levels of SAPT, the MAE values for dispersion for jun-cc-pVDZ are consistently near 1.0 kcal mol⁻¹, with nearly errors all leading to underbinding, and with very large error distributions. Increasing the basis set to aug-cc-pVDZ substantially narrows the error distributions, and reduces the MAEs to between roughly 0.2 and 0.5 kcal mol⁻¹ depending on the level of theory. Methods that only use E_{disp}⁽²⁰⁾ + E_{exch-disp}⁽²⁰⁾ (SAPT0 and sSAPT0) still exhibit a fairly broad distribution of errors, but with a much more modest bias towards underbinding than with the jun-cc-pVDZ basis. Increasing the level of theory results in more narrow error distributions that are less biased towards underbinding; mean absolute errors are reduced by about a factor of 2 or more. Further increasing the basis set to aug-cc-pVTZ causes additional significant reduction in dispersion energy errors for most of the SAPT levels, and a further tightening of the error distributions. All of the methods beyond SAPT2 have MAE of 0.13 kcal mol⁻¹ or less, except SAPT2+(3)(CCD) (MAE 0.16 kcal mol⁻¹).

Figure 8 presents a similar analysis of the errors in the energy components, for the 358-dimer subset for which we were able to obtain aug-cc-pVQZ results. Error statistics like MAE are somewhat worse for this subset than for the full 4569-dimer test set, because many of the dimers in the subset are more strongly interacting (doubly H-bonded dimers from HBC6, and ion-containing systems from Ion38). Generally speaking, the error statistics are not improved, or only very slightly improved, as the basis set is increased from aug-cc-pVTZ to aug-cc-pVQZ. Notable exceptions are for exchange energies for SAPT2 and beyond, and SAPT2+(CCD) dispersion. For SAPT2+3, dispersion energies actually get very slightly worse in the aug-cc-pVQZ basis vs the SAPT2+3(CCD)/aug-cc-pVQZ values.

Figures S17 and S18 in the Supplemental Information present similar information as Figures 7 and 8, but extended to

FIG. 7. Mean absolute errors, root mean square errors, minimum and maximum errors (kcal mol^{-1}), MCUREs (%), and distributions of errors via violin plots for interaction energy components at selected levels of SAPT with respect to SAPT2+3(CCD)/aug-cc-pVTZ. Results shown for the SSI, S66x8, HBC6, NBC10ext, X31x10, and Ion38 databases for a total of 4569 dimers.

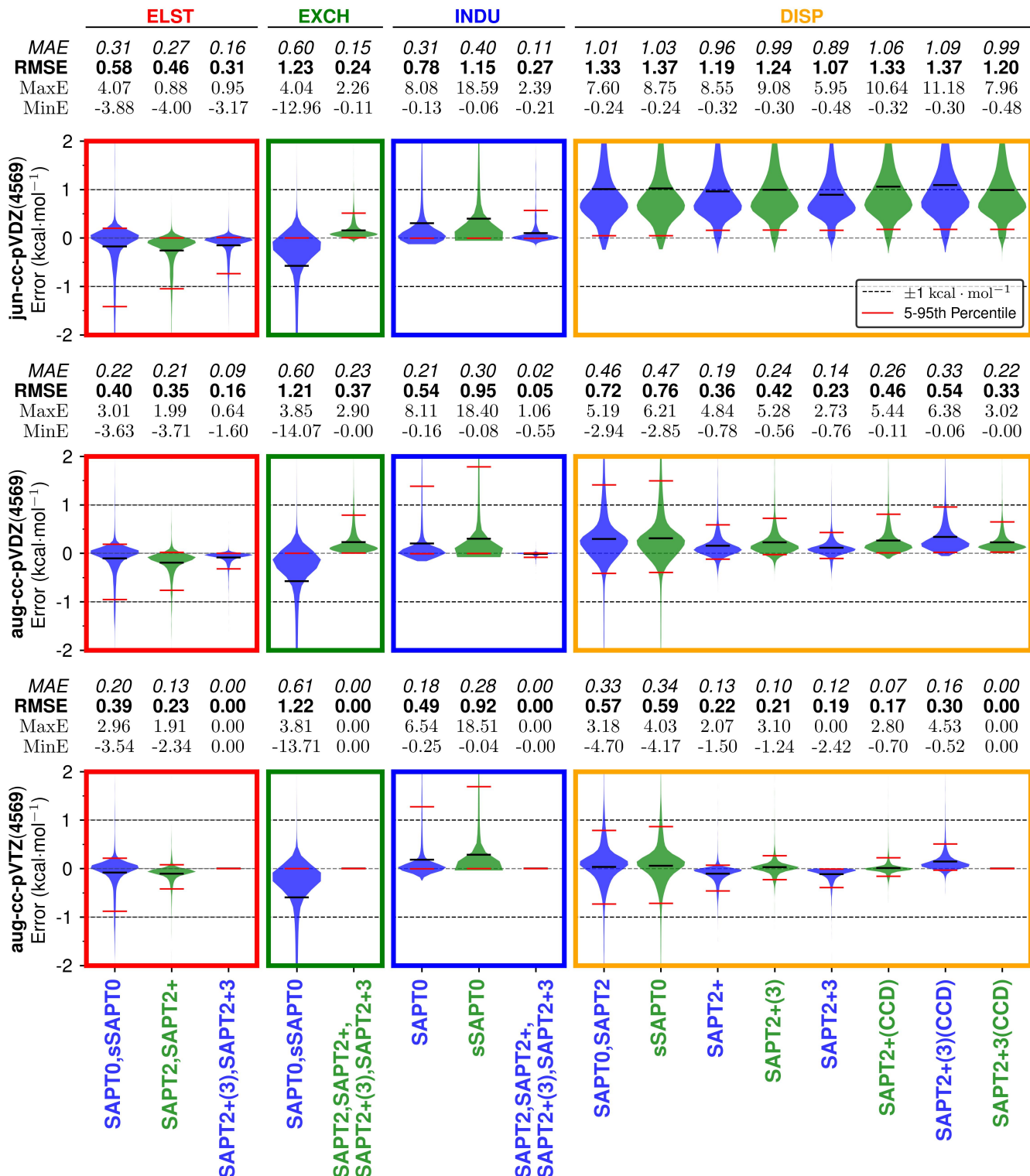
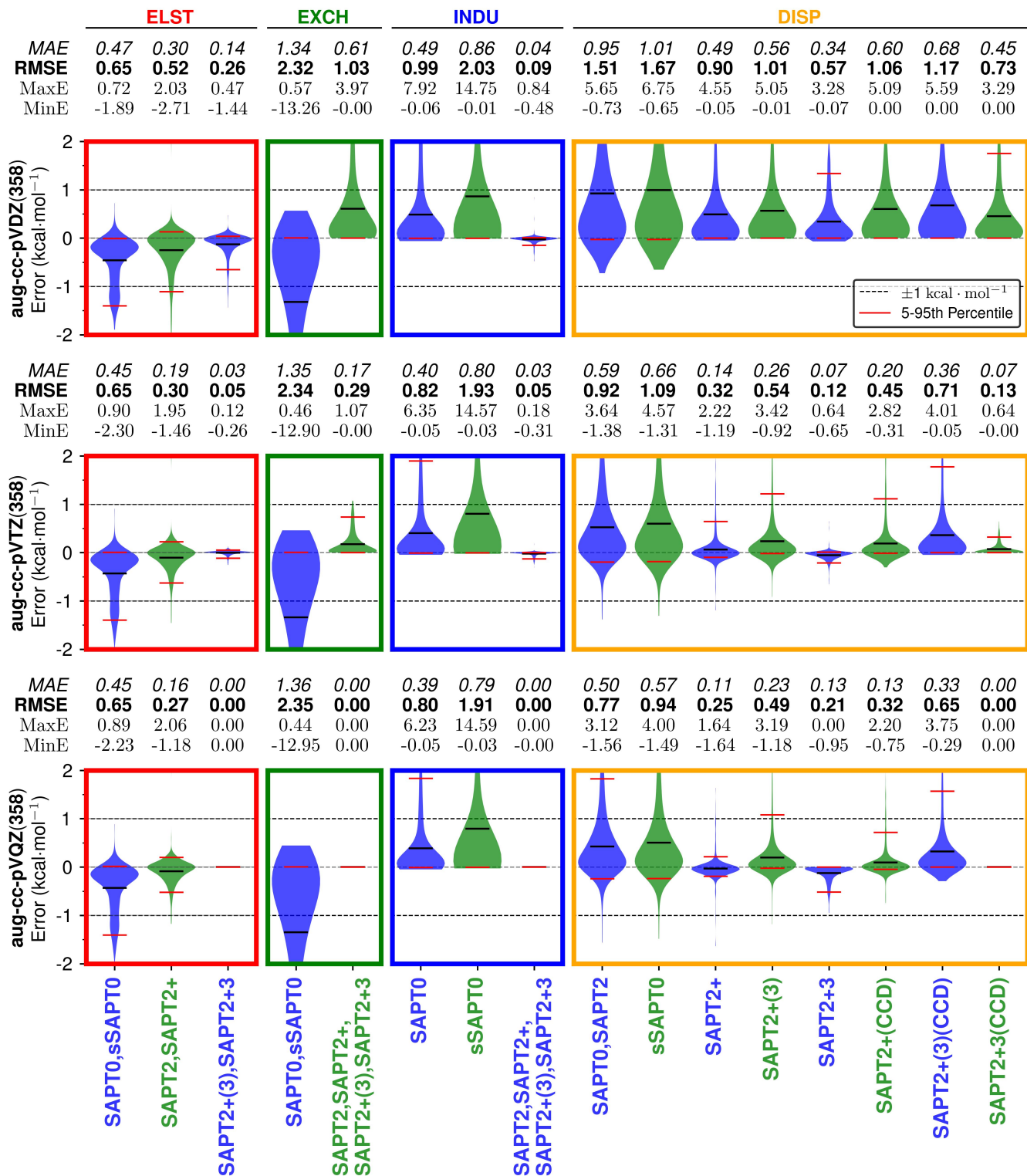


FIG. 8. Mean absolute errors, root mean square errors, minimum and maximum errors (kcal mol^{-1}), MCUREs (%), and distributions of errors via violins for interaction energy components at selected levels of SAPT with respect to SAPT2+3(CCD)/aug-cc-pVQZ. Interaction energies are computed for the HBC6, Ion38, and a subset of the S66x8 datasets for a total of 358 dimers.



include basis set extrapolated values. As we observed above for total interaction energies, two-point extrapolation of terms depending on electron correlation is effective for SAPT. Figure S18 demonstrates that aug-cc-pV[DT]Z values are very close to those from aug-cc-pVQZ, and for certain dispersion terms, they are actually closer to the CBS limit. This is perhaps surprising given that, in more general contexts, double- ζ basis sets are not always sufficiently large for effective two-point extrapolation of correlation energies; the correction can sometimes overshoot the CBS limit. On the other hand, there is only minor improvement seen in moving from aug-cc-pVTZ results to aug-cc-pV[DT]Z results. This is consistent with the very minor improvements seen in Figure 8 upon improving the basis set from aug-cc-pVTZ to aug-cc-pVQZ. The biggest improvements shown for the full 4569-dimer dataset upon moving from aug-cc-pVTZ to aug-cc-pV[DT]Z are an elimination of a 0.09 kcal mol⁻¹ MAE and 0.15 kcal mol⁻¹ RMSE for higher-order exchange energies, and an elimination of a 0.09 kcal mol⁻¹ and 0.14 kcal mol⁻¹ RMSE for SAPT2+3(CCD) dispersion. Improvements from aug-cc-pVQZ to aug-cc-pV[TD]Z for the 358-dimer subset in Figure S18 are more modest, but higher-order exchange still benefits from an elimination of a 0.12 kcal mol⁻¹ MAE, and several dispersion energies have their MAEs reduced by \sim 0.05 kcal mol⁻¹ and their RMSEs by \sim 0.1 kcal mol⁻¹.

SAPT0 is known to strongly overbind some dimers, particularly those featuring π - π interactions.¹² We have attributed this to the simplistic treatment of electron correlation in SAPT0 dispersion, which is essentially an intermolecular MP2 dispersion (it is also called “uncoupled” dispersion in the literature). For these systems, larger basis sets just exaggerate the problem and lead to even stronger overbinding. It is perhaps surprising, then, that on average over the present large test set, the SAPT0 dispersion error statistics are actually improved at each step as one progresses to larger basis sets, from jun-cc-pVDZ through aug-cc-pVQZ. We expect that π interactions are not prevalent enough in the test set to show worse results for larger basis sets. To check on this hypothesis, the Supplementary Material presents similar interaction energy component error distributions, broken down into different subsets of dimers. Results for the NBC10ext test set, which features numerous π and π - π interactions, indeed show worse results for SAPT0 dispersion as the basis set is increased (see Fig. S25).

To better understand the extent of error cancellations in each level of SAPT, we show mean errors (ME) of total and component energies in kcal mol⁻¹ plotted for all levels of SAPT using jun-cc-pVDZ, aug-cc-pVDZ, and aug-cc-pVTZ in Figure 9 (note the larger y-axis scale in the subplot for jun-cc-pVDZ). This Figure differs from Figure 5 in that errors are now evaluated relative to SAPT2+3(CCD) δ MP2/aug-cc-pVTZ values, rather than against the same level of SAPT in the aug-cc-pVQZ basis. For SAPT2+ δ MP2 through SAPT2+(3) δ MP2 (with or without CCD dispersion), the δE_{MP2} error is evaluated as the difference between the computed value of $\delta E_{\text{MP2}}^{[2]}$ and the reference value $\delta E_{\text{MP2}}^{[3]}$ /aug-cc-pVTZ. For SAPT methods without a δE_{MP2} correction, the δE_{MP2} error is considered to be the entirety of the $\delta E_{\text{MP2}}^{[3]}$ /aug-

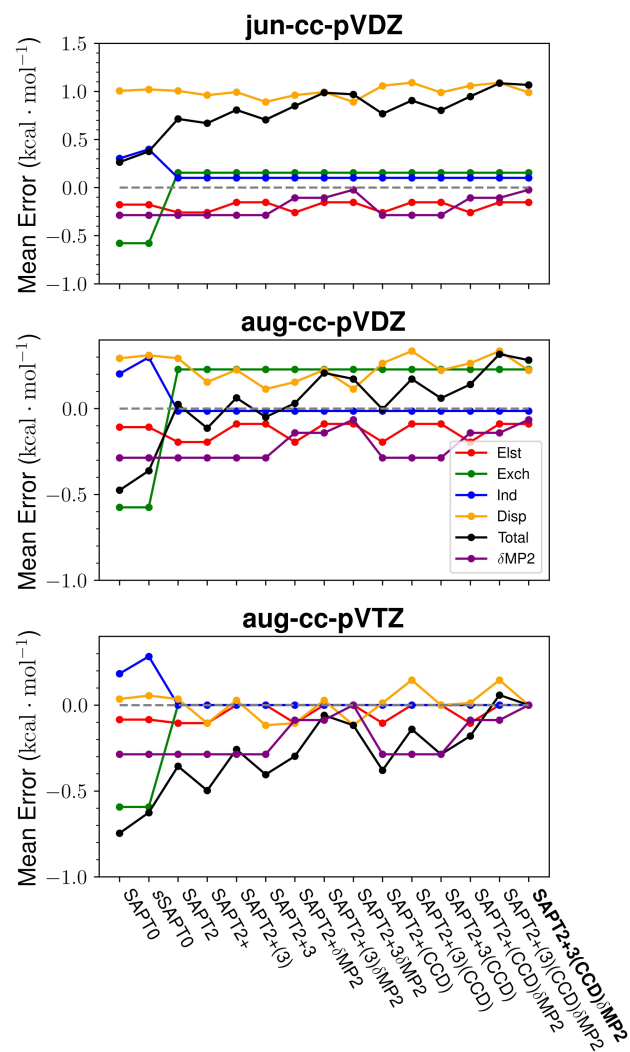


FIG. 9. Mean errors (kcal mol⁻¹) of SAPT components computed on our entire dimer database (4569 dimers) with jun-cc-pVDZ, aug-cc-pVDZ and aug-cc-pVTZ basis sets. MEs are computed with respect to SAPT2+3(CCD) δ MP2/aug-cc-pVTZ.

cc-pVTZ reference value.

Although the electrostatics contribution is fairly accurate across all SAPT methods and basis sets considered, Figure 9 helps demonstrate that the good accuracy of several SAPT levels for total interaction energies in smaller basis sets tends to rely on a cancellation of errors between the remaining energy components. For SAPT0, positive-signed exchange is substantially underestimated in all basis sets, leading to significant negative errors; thus, the accuracy of SAPT0 in double- ζ basis sets relies on the observed significant counterbalancing underestimation of the magnitude of negative-signed dispersion (positive errors in dispersion) and additional positive errors in induction.

SAPT2+/aug-cc-pVDZ shows very good total interaction energies, and we continue to recommend its use as a medium-cost SAPT variant. Nonetheless, it underestimates the mag-

nitude of negative dispersion energies and overestimates the strength of positive exchange energies (both yielding positive errors), which is partially cancelled by an overestimation of the magnitude of stabilizing electrostatic effects (slight negative errors) and an additional negative error from the lack of a δE_{MP2} correction relative to the reference level of theory for this Figure. The main benefit in moving from SAPT0/aug-cc-pVDZ to SAPT2+/aug-cc-pVDZ is a substantial reduction in the magnitude of the mean error for exchange, with a smaller reduction in the magnitude of the mean error in dispersion, and a significant reduction in the magnitude of the mean error in the total interaction energy.

In the aug-cc-pVTZ basis, errors in exchange and induction go to zero (by definition) for SAPT2 and beyond in this comparison vs SAPT2+3(CCD) δ MP2/aug-cc-pVTZ, and they are very small for electrostatics at all levels of SAPT. Mean errors in dispersion are also typically quite small (between $\pm 0.1 \text{ kcal mol}^{-1}$), although occasionally a little outside this range. Thus, the mean errors in total interaction energy are largely governed by the errors in dispersion (and to a lesser extent, electrostatics), and the presence or absence of a δE_{MP2} correction, which has a greater effect than any other improvement for SAPT2 and beyond in the aug-cc-pVTZ basis.

Highlighted in Figure 9, we see that all errors converge quite tightly around SAPT2+(3) δ MP2/aug-cc-pVTZ, the previously named “gold” SAPT level; results are very close to those of the most complete method considered in this Figure, SAPT2+3(CCD) δ MP2/aug-cc-pVTZ, but are significantly easier to compute. Further, we know from the results presented in Figure 8 that using a larger basis set as the reference would not substantially change these conclusions.

C. δ -corrected Dispersion

Our analysis demonstrates the relatively slow convergence of dispersion, compared to the other components, with respect to basis set. As a result, to approach the accuracy of SAPT in a larger basis set, one needs first to apply some sort of basis set correction to dispersion. Furthermore, computation of dispersion is by far the most time-consuming part of a SAPT computation. In Figure 10, we present wall times for all terms in a SAPT2+3(CCD) δ MP2 computation for the water dimer and benzene dimer in aug-cc-pVTZ and aug-cc-pVQZ basis sets. Computation of CCD amplitudes and computation of the amplitudes in $E_{\text{disp}}^{(30)}$ are the most expensive terms, with (T) terms also showing a moderate cost. Clearly, these terms show the most drastically unfavorable scaling with respect to basis set, at times showing over a 10x increase in wall time when going from aug-cc-pVTZ to aug-cc-pVQZ.

In light of the high cost of dispersion and its slow convergence with respect to basis set, we propose a focal point^{68,69} (δ -corrected or composite) dispersion that uses the less expensive SAPT0 dispersion to compute a basis set correction for the costly CCD-based dispersion. For small (S) and large

(L) basis sets, we define our dispersion correction as

$$\delta E_{\text{disp}}^{\text{SL}} = (E_{\text{disp}}^{(20)}[\text{L}] + E_{\text{exch-disp}}^{(20)}[\text{L}]) - (E_{\text{disp}}^{(20)}[\text{S}] + E_{\text{exch-disp}}^{(20)}[\text{S}]), \quad (22)$$

which is simply the difference in SAPT0 dispersion for large and small basis sets. The cost of this correction is roughly equivalent to SAPT0 dispersion in the larger basis set, which we have shown is still less expensive than the higher-order terms in the smaller basis set. Our approach is completely analogous to the common practice of using large-basis MP2 to correct CCSD(T) computations in smaller basis sets.¹⁰² In the context of SAPT, earlier works have noticed this large basis set dependence of $E_{\text{disp}}^{(2)}$ and have used an explicitly correlated Gaussian geminal basis to acquire accurate dispersion energies for small dimers.^{103–107}

In Figure 11 we show MAEs and error distributions for post-SAPT0 dispersion energies, using the aug-cc-pVDZ basis set (error distributions in blue), and those same methods including $\delta E_{\text{disp}}^{\text{DT}}$ corrections (in green). For all cases except SAPT2+3, the δE_{disp} correction substantially improves the error distributions, sometimes dramatically, as in the case of SAPT2+3(CCD). Thus, for just the extra cost of computing $E_{\text{disp}}^{(20)} + E_{\text{exch-disp}}^{(20)}$ in the aug-cc-pVTZ basis (and these terms are rather efficient in our density fitting algorithm, see again Fig. 10), dispersion energies are nicely improved. The correction $E_{\text{disp}}^{\text{DT}}$ tends to be negative, shifting the error distributions down in the Figure. This is beneficial, as in the aug-cc-pVDZ basis, most dispersion energies are not negative enough. The $\delta E_{\text{disp}}^{\text{DT}}$ correction tends to bring the mean errors in the dispersion error distributions from positive to close to zero. Occasionally it overcorrects and makes the mean error slightly negative, such as for SAPT2+3 $\delta E_{\text{disp}}^{\text{DT}}$, where the corrected values have essentially the same MAE and RMSD, but the mean error has shifted from positive to negative. Figure S19 of the Supplementary Material presents similar information for our 358-dimer subset, which in general contains more challenging test cases. The improvement afforded by $\delta E_{\text{disp}}^{\text{DT}}$ is even more significant for those systems. Figure S21 of the Supplemental Material then examines $E_{\text{disp}}^{\text{TQ}}$ corrections for the subset, where aug-cc-pVQZ results are available. The correction is again beneficial in nearly all cases, although the improvement is smaller because SAPT/aug-cc-pVTZ dispersion values have less remaining basis set error.

Given the discussion above about cancellation of errors, it is also worth examining whether this improvement in dispersion energies tends to improve or degrade accuracy for total interaction energies. Figure 12 provides error distributions for all levels of SAPT considered here in the aug-cc-pVDZ basis, with (green) and without (blue) $\delta E_{\text{disp}}^{\text{DT}}$ corrections. Favorable error cancellations at the SAPT/aug-cc-pVDZ level are spoiled in some cases [SAPT0, SAPT2+, SAPT2+3], and overall error statistics are about the same in some other cases [SAPT2, SAPT2+(CCD)]. However, in the other cases, the correction leads to a significant improvement. In the case of SAPT2+3(CCD) δ MP2, the MAE and RMSE are reduced from 0.40 and 0.63 kcal mol^{-1} to 0.15 and 0.30 kcal mol^{-1} , making SAPT2+3(CCD) δ MP2+ $\delta E_{\text{disp}}^{\text{DT}}$ more ac-

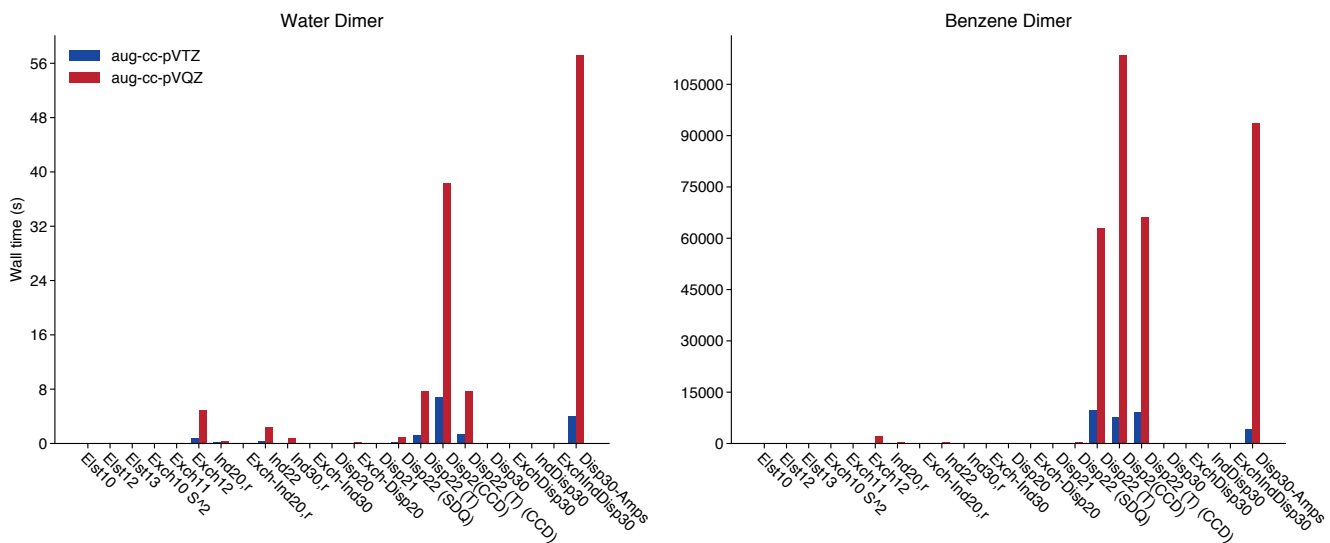


FIG. 10. Wall times of all SAPT components. Timings are obtained for the water dimer and the benzene dimer, using both aug-cc-pVTZ and aug-cc-pVQZ basis sets. Timings were recorded using 6 cores of an Intel i9-10980XE chip with a 3.00GHz clock speed.

curate on average than any SAPT/aug-cc-pVDZ method without δE_{disp} correction. Several of the other $\delta E_{\text{disp}}^{\text{DT}}$ -corrected methods are even more accurate on average (lower MAE and RMSE): SAPT2+(3) δ MP2 $\delta E_{\text{disp}}^{\text{DT}}$, SAPT2+3 δ MP2 $\delta E_{\text{disp}}^{\text{DT}}$, and SAPT2+(CCD) δ MP2 $\delta E_{\text{disp}}^{\text{DT}}$, with MAE values of 0.11–0.12 kcal mol⁻¹ and RMSE values of 0.20–0.24 kcal mol⁻¹. The latter four levels of theory all share the same errors in induction (aug-cc-pVDZ component error distributions shown in Fig. 7), but the SAPT methods including third-order terms in v (SAPT2+(3) and SAPT2+3 type methods) show reduced errors in electrostatics (Fig. 7). Given the substantial increase in computational expense associated with the computation of the the terms that enter SAPT at the “+3” level, or those involved in (CCD) dispersion (see again Fig. 10), SAPT2+(3) δ MP2 $\delta E_{\text{disp}}^{\text{DT}}$ seems very promising as a method with excellent error cancellation for total interaction energies, low component errors, and lower computational cost compared to higher levels of SAPT or larger basis sets.

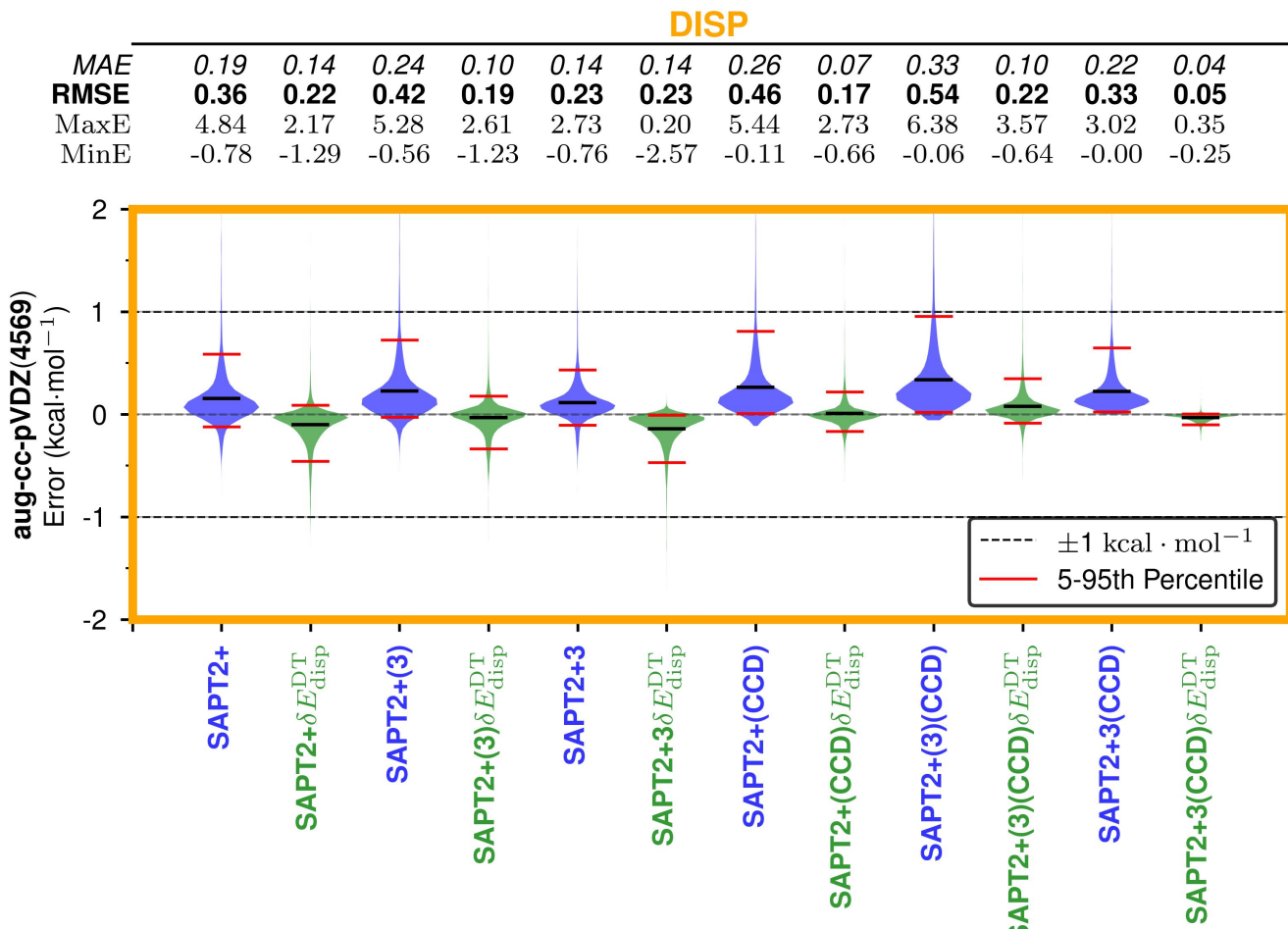
Figure S22 of the Supplemental Material presents similar information for the 358-dimer subset, adding $\delta E_{\text{disp}}^{\text{TQ}}$ corrections to aug-cc-pVTZ SAPT results. Here, the δE_{disp} correction is generally not beneficial, which is consistent with the generally larger errors seen for most SAPT methods considered here if the basis is increased from aug-cc-pVTZ to aug-cc-pVQZ; only the very highest levels of SAPT see a benefit from this basis set increase (see Figs. 1–4). SAPT2+(3)(CCD) δ MP2 and SAPT2+3(CCD) δ MP2 do show modest improvements upon $\delta E_{\text{disp}}^{\text{TQ}}$ correction, consistent with their improved accuracy in the aug-cc-pVQZ basis set vs the aug-cc-pVTZ basis.

IV. SUMMARY AND CONCLUSIONS

SAPT is a valuable tool for gaining quantitative and qualitative insight to the nature of intermolecular interactions. Crucial to the utility of SAPT is its natural decomposition into physically-meaningful components: electrostatics, exchange-repulsion, induction, and dispersion. In our previous work,³⁴ we analyzed the accuracy and efficiency of SAPT in a variety of basis sets, paying exclusive attention to the total interaction energies. In that work, we identified three combinations of SAPT methods and basis sets, for low to high computational cost, that provided good error statistics and good accuracy/cost ratios.

In this work, we revisit a systematic analysis of wave function-based SAPT methods with the goals of (a) re-evaluating our conclusions based on a much larger dataset and (b) evaluating each level of SAPT based on both total and component energies. We assessed total interaction energies using CCSD(T)/CBS reference values, and we evaluated the component energies using SAPT2+3(CCD)/aug-cc-pVTZ results as reference values for our entire 4569-dimer dataset, and larger-basis SAPT2+3(CCD)/aug-cc-pVQZ components as reference values for a limited subset of 358 dimers. Our previous recommendations of SAPT2+/aug-cc-pVDZ and SAPT2+(3) δ MP2/aug-cc-pVTZ as “silver” and “gold” levels of SAPT remain unchanged. For SAPT2+(3), all component energies are evaluated at the highest level we have implemented except for dispersion; in an aug-cc-pVTZ basis, the dispersion MAE vs the SAPT2+3(CCD) level is only 0.10 kcal mol⁻¹. For the more challenging dimers of the 358-dimer subset, SAPT2+(3)/aug-cc-pVTZ components are all within 0.3 kcal mol⁻¹ MAE of SAPT2+3(CCD)/aug-cc-pVQZ values (dispersion having the largest error). The MAE for SAPT2+(3)/aug-cc-pVTZ is only 0.18 kcal mol⁻¹ vs CCSD(T)/CBS for the full test set, and this is re-

FIG. 11. Mean absolute errors, root mean square errors, minimum and maximum errors (kcal mol^{-1}), and distributions of dispersion interaction energy errors (kcal mol^{-1}) via violins of selected levels of SAPT with and without the δ -corrected dispersion ($\delta E_{\text{disp}}^{\text{DT}}$). Errors are computed using SAPT2+3(CCD)/aug-cc-pVTZ dispersion as the reference for the SSI, S66x8, HBC6, NBC10ext, X31x10, and Ion38 databases totaling 4569 dimer geometries.



duced to 0.11 kcal mol^{-1} if a δMP2 correction is added [SAPT2+3 δMP2 /aug-cc-pVTZ].

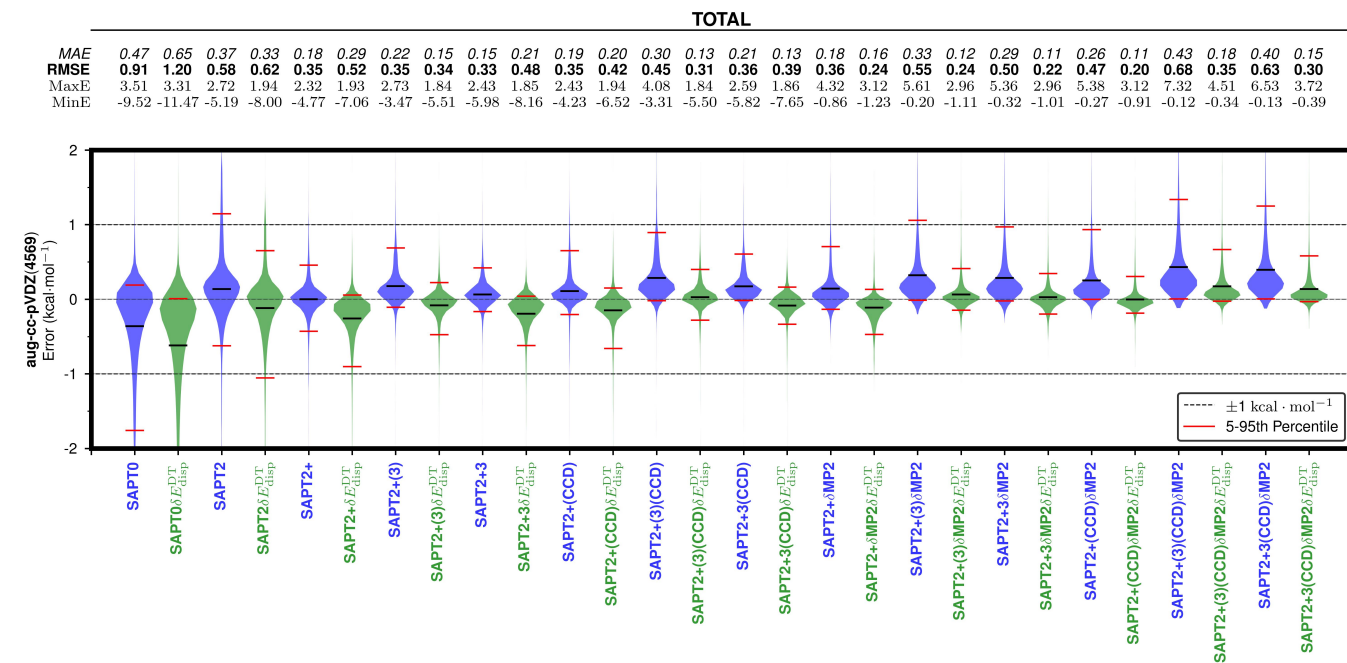
The excellent agreement seen here between the highest levels of SAPT, and between high-level SAPT and CCSD(T)/CBS for total interaction energies, suggests that the hierarchy of SAPT methods considered here is converging fairly well towards the electron correlation and basis set limits by the time the highest SAPT levels and the aug-cc-pVTZ or aug-cc-pVQZ basis sets are used. This, in turn, suggests that higher levels of SAPT with larger basis sets should be suitable for benchmarks in developing SAPT-based force fields and intermolecular potentials.

In our previous work, we recommended *s*SAPT0/jun-cc-pVDZ as the “bronze” level SAPT, i.e., the best low-cost SAPT available. Looking at our larger dataset, which now includes the sidechain-sidechain interaction (SSI) database, we found SAPT0/aug-cc-pVDZ to be the preferred low-cost SAPT, though *s*SAPT0/jun-cc-pVDZ did show better accu-

racy for dimers at close range or with strong hydrogen bonds. We found that both methods rely strongly on cancellation of errors, though *s*SAPT0/jun-cc-pVDZ dispersion was substantially less accurate in comparison to SAPT0/aug-cc-pVDZ dispersion. In fact, all SAPT0 components perform better in the aug-cc-pVDZ basis than they do in jun-cc-pVDZ, with SAPT0 also outperforming *s*SAPT0. Therefore, we recommend SAPT0/aug-cc-pVDZ for applications to large molecules, or for generating very large datasets for use in fitting intermolecular potentials, where higher levels of SAPT may be infeasible. Despite the improved treatment of dispersion in SAPT0/aug-cc-pVDZ over *s*SAPT0/jun-cc-pVDZ, we recognize the possibility that *s*SAPT0/jun-cc-pVDZ may still be preferable for applications involving strongly interacting systems.^{80,81}

Among the interaction energy components, arguably dispersion is the most difficult to converge with respect to level of theory and basis set. Consistent with prior work,³⁴ inclu-

FIG. 12. Mean absolute errors, root mean square errors, minimum and maximum errors (kcal mol^{-1}), and distributions of total interaction energy errors (kcal mol^{-1}) via violins of selected levels of SAPT with and without the δ -corrected dispersion ($\delta E_{\text{disp}}^{\text{DT}}$). Errors are computed using CCSD(T)/CBS interaction energies as the reference for the SSI, S66x8, HBC6, NBC10ext, X31x10, and Ion38 databases totaling 4569 dimer geometries.



knowledges support from the U.S. National Science Foundation Graduate Research Fellowship, Grant No. DGE-2039655.

AUTHOR DECLARATIONS

The authors have no conflicts to disclose.

DATA AVAILABILITY

The data that support the findings of this study are available within the article and its supplementary material.

- ¹K. E. Riley and P. Hobza, "Noncovalent interactions in biochemistry," *WIREs Comput. Mol. Sci.* **1**, 3–17 (2011).
- ²C. D. Sherrill, "Energy component analysis of π interactions," *Acc. Chem. Res.* **46**, 1020–1028 (2013).
- ³Pastorcak, Ewa and Corminboeuf, Clémence, "Perspective: Found in translation: Quantum chemical tools for grasping non-covalent interactions," *J. Chem. Phys.* **146**, 120901 (2017).
- ⁴J. Hoja, A. M. Reilly, and A. Tkatchenko, "First-principles modeling of molecular crystals: structures and stabilities, temperature and pressure," *WIREs Comput. Mol. Sci.* **7**, e1294 (2017).
- ⁵Y. S. Al-Hamdani and A. Tkatchenko, "Understanding non-covalent interactions in larger molecular complexes from first principles," *J. Chem. Phys.* **150**, 010901 (2019).
- ⁶E. A. Meyer, R. K. Castellano, and F. Diederich, "Interactions with aromatic rings in chemical and biological recognition," *Angew Chem Int Ed Engl* **42**, 1210–1250 (2003).
- ⁷R. M. Parrish, D. F. Sitkoff, D. L. Cheney, and C. D. Sherrill, "The Surprising Importance of Peptide Bond Contacts in Drug-Protein Interactions," *Chemistry* **23**, 7887–7890 (2017).
- ⁸G. Hill, G. Forde, N. Hill, W. A. Lester, W. A. Sokalski, and J. Leszczynski, "Interaction energies in stacked DNA bases? How important are electrostatics?" *Chem. Phys. Lett.* **381**, 729–732 (2003).
- ⁹T. M. Parker, E. G. Hohenstein, R. M. Parrish, N. V. Hud, and C. D. Sherrill, "Quantum-mechanical analysis of the energetic contributions to π stacking in nucleic acids versus rise, twist, and slide," *JACS* **135**, 1306–1316 (2013).
- ¹⁰K. Raghavachari, G. W. Trucks, J. A. Pople, and M. Head-Gordon, "A fifth-order perturbation comparison of electron correlation theories," *Chem. Phys. Lett.* **157**, 479–483 (1989).
- ¹¹J. Řezáč and P. Hobza, "Describing Noncovalent Interactions beyond the Common Approximations: How Accurate Is the "Gold Standard," CCSD(T) at the Complete Basis Set Limit?" *J. Chem. Theor. Comput.* **9**, 2151–2155 (2013).
- ¹²C. D. Sherrill, T. Takatani, and E. G. Hohenstein, "An Assessment of Theoretical Methods for Nonbonded Interactions: Comparison to Complete Basis Set Limit Coupled-Cluster Potential Energy Curves for the Benzene Dimer, the Methane Dimer, Benzene-Methane, and Benzene-H₂S," *J. Phys. Chem. A* **113**, 10146–10159 (2009).
- ¹³J. Lee and M. Head-Gordon, "Regularized Orbital-Optimized Second-Order Møller-Plesset Perturbation Theory: A Reliable Fifth-Order-Scaling Electron Correlation Model with Orbital Energy Dependent Regularizers," *J. Chem. Theor. Comput.* **14**, 5203–5219 (2018).
- ¹⁴J. Shee, M. Loipersberger, A. Rettig, J. Lee, and M. Head-Gordon, "Regularized Second-Order Møller-Plesset Theory: A More Accurate Alternative to Conventional MP2 for Noncovalent Interactions and Transition Metal Thermochemistry for the Same Computational Cost," *J. Phys. Chem. Lett.* **12**, 12084–12097 (2021).
- ¹⁵M. Loipersberger, L. W. Bertels, J. Lee, and M. Head-Gordon, "Exploring the Limits of Second- and Third-Order Møller-Plesset Perturbation Theories for Noncovalent Interactions: Revisiting MP2.5 and Assessing the Importance of Regularization and Reference Orbitals," *J. Chem. Theor. Comput.* **17**, 5582–5599 (2021).
- ¹⁶S. Grimme, "Accurate description of van der Waals complexes by density functional theory including empirical corrections," *J. Comput. Chem.* **25**, 1463–1473 (2004).
- ¹⁷S. Grimme, "Semiempirical GGA-type density functional constructed with a long-range dispersion correction," *J. Comput. Chem.* **27**, 1787–1799 (2006).
- ¹⁸S. Grimme, J. Antony, S. Ehrlich, and H. Krieg, "A consistent and accurate ab initio parametrization of density functional dispersion correction (DFT-D) for the 94 elements H–Pu," *J. Chem. Phys.* **132**, 154104 (2010).
- ¹⁹S. Grimme, "Density functional theory with London dispersion corrections," *WIREs Comput. Mol. Sci.* **1**, 211–228 (2011).
- ²⁰S. Grimme, S. Ehrlich, and L. Goerigk, "Effect of the damping function in dispersion corrected density functional theory," *J. Comp. Chem.* **32**, 1456–1465 (2011).
- ²¹E. Caldeweyher, C. Bannwarth, and S. Grimme, "Extension of the D3 dispersion coefficient model," *J. Chem. Phys.* **147**, 034112 (2017).
- ²²E. Caldeweyher, J.-M. Mewes, S. Ehler, and S. Grimme, "Extension and evaluation of the D4 London-dispersion model for periodic systems," *Phys. Chem. Chem. Phys.* **22**, 8499–8512 (2020).
- ²³S. Grimme, J. Antony, T. Schwabe, and C. Mück-Lichtenfeld, "Density functional theory with dispersion corrections for supramolecular structures, aggregates, and complexes of (bio)organic molecules," *Org. Biomol. Chem.* **5**, 741–758 (2007).
- ²⁴K. Kitaura and K. Morokuma, "A new energy decomposition scheme for molecular interactions within the Hartree-Fock approximation," *Int. J. Quant. Chem.* **10**, 325–340 (1976).
- ²⁵W. Chen and M. S. Gordon, "Energy decomposition analyses for many-body interaction and applications to water complexes," *J. Phys. Chem.* **100**, 14316–14328 (1996).
- ²⁶E. D. Glendening and A. Streitwieser, "Natural energy decomposition analysis: An energy partitioning procedure for molecular interactions with application to weak hydrogen bonding, strong ionic, and moderate donor–acceptor interactions," *J. Chem. Phys.* **100**, 2900 (1998).
- ²⁷R. Z. Khalilullin, E. A. Cobar, R. C. Lochan, A. T. Bell, and M. Head-Gordon, "Unravelling the origin of intermolecular interactions using absolutely localized molecular orbitals," *J. Phys. Chem. A* **111**, 8753–8765 (2007).
- ²⁸J. Thirman and M. Head-Gordon, "An energy decomposition analysis for second-order Møller-Plesset perturbation theory based on absolutely localized molecular orbitals," *J. Chem. Phys.* **143**, 084124 (2015).
- ²⁹P. R. Horn, Y. Mao, and M. Head-Gordon, "Probing non-covalent interactions with a second generation energy decomposition analysis using absolutely localized molecular orbitals," *Phys. Chem. Chem. Phys.* **18**, 23067–23079 (2016).
- ³⁰W. B. Schneider, G. Bistoni, M. Sparta, M. Saitow, C. Ripplinger, A. A. Auer, and F. Neese, "Decomposition of Intermolecular Interaction Energies within the Local Pair Natural Orbital Coupled Cluster Framework," *J. Chem. Theor. Comput.* **12**, 4778–4792 (2016).
- ³¹B. Jeziorski, R. Moszynski, and K. Szalewicz, "Perturbation-Theory Approach to Intermolecular Potential-Energy Surfaces of Van-Der-Waals Complexes," *Chem. Rev.* **94**, 1887–1930 (1994).
- ³²K. Szalewicz, "Symmetry-adapted perturbation theory of intermolecular forces," *WIREs Comput. Mol. Sci.* **2**, 254–272 (2012).
- ³³K. Patkowski, "Recent developments in symmetry-adapted perturbation theory," *WIREs Comput. Mol. Sci.* **10**, e1452 (2019).
- ³⁴T. M. Parker, L. A. Burns, R. M. Parrish, A. G. Ryno, and C. D. Sherrill, "Levels of symmetry adapted perturbation theory (SAPT). I. Efficiency and performance for interaction energies," *J. Chem. Phys.* **140**, 094106 (2014).
- ³⁵E. G. Hohenstein, R. M. Parrish, C. D. Sherrill, J. M. Turney, and H. F. Schaefer, "Large-scale symmetry-adapted perturbation theory computations via density fitting and Laplace transformation techniques: investigating the fundamental forces of DNA-intercalator interactions," *J. Chem. Phys.* **135**, 174107 (2011).
- ³⁶A. J. Misquitta, R. Podeszwa, B. Jeziorski, and K. Szalewicz, "Intermolecular potentials based on symmetry-adapted perturbation theory with dispersion energies from time-dependent density-functional calculations," *J. Chem. Phys.* **123**, 214103 (2005).
- ³⁷J. G. McDaniel, K. Yu, and J. R. Schmidt, "Ab Initio, Physically Motivated Force Fields for CO₂ Adsorption in Zeolitic Imidazolate Frameworks," *J. Chem. Phys.*

- Phys. Chem. C **116**, 1892–1903 (2012).
- ³⁸J. G. McDaniel and J. R. Schmidt, “Physically-Motivated Force Fields from Symmetry-Adapted Perturbation Theory,” J. Phys. Chem. A **117**, 2053–2066 (2013).
- ³⁹M. J. Van Vleet, A. J. Misquitta, and J. R. Schmidt, “New Angles on Standard Force Fields: Toward a General Approach for Treating Atomic-Level Anisotropy.” J. Chem. Theor. Comput. **14**, 739–758 (2018).
- ⁴⁰S. Naseem-Khan, N. Gresh, A. J. Misquitta, and J.-P. Piquemal, “Assessment of SAPT and Supermolecular EDA Approaches for the Development of Separable and Polarizable Force Fields.” J. Chem. Theor. Comput. **17**, 2759–2774 (2021).
- ⁴¹D. P. Metcalf, A. Koutsoukas, S. A. Spronk, B. L. Claus, D. A. Loughney, S. R. Johnson, D. L. Cheney, and C. D. Sherrill, “Approaches for machine learning intermolecular interaction energies and application to energy components from symmetry adapted perturbation theory.” J. Chem. Phys. **152**, 074103 (2020).
- ⁴²Z. L. Glick, D. P. Metcalf, A. Koutsoukas, S. A. Spronk, D. L. Cheney, and C. D. Sherrill, “AP-Net: An atomic-pairwise neural network for smooth and transferable interaction potentials.” J. Chem. Phys. **153**, 044112 (2020).
- ⁴³J. B. Schriber, D. R. Nascimento, A. Koutsoukas, S. A. Spronk, D. L. Cheney, and C. D. Sherrill, “CLIFF: A component-based, machine-learned, intermolecular force field.” J. Chem. Phys. **154**, 184110 (2021).
- ⁴⁴J. A. Rackers, Q. Wang, C. Liu, J.-P. Piquemal, P. Ren, and J. W. Ponder, “An optimized charge penetration model for use with the AMOEBA force field.” Phys. Chem. Chem. Phys. **19**, 276–291 (2017).
- ⁴⁵J. A. Rackers, C. Liu, P. Ren, and J. W. Ponder, “A physically grounded damped dispersion model with particle mesh Ewald summation.” J. Chem. Phys. **149**, 084115 (2018).
- ⁴⁶J. A. Rackers and J. W. Ponder, “Classical Pauli repulsion: An anisotropic, atomic multipole model.” J. Chem. Phys. **150**, 084104 (2019).
- ⁴⁷H. L. Williams, K. Szalewicz, R. Moszynski, and B. Jeziorski, “Dispersion energy in the coupled pair approximation with noniterative inclusion of single and triple excitations.” J. Chem. Phys. **103**, 4586 (1995).
- ⁴⁸A. Li, H. S. Muddana, and M. K. Gilson, “Quantum Mechanical Calculation of Noncovalent Interactions: A Large-Scale Evaluation of PMx, DFT, and SAPT Approaches.” J. Chem. Theor. Comput. **10**, 1563–1575 (2014).
- ⁴⁹H. L. Williams and C. Chabalowski, “Using Kohn-Sham orbitals in symmetry-adapted perturbation theory to investigate intermolecular interactions.” J. Phys. Chem. **105**, 646–659 (2001).
- ⁵⁰A. J. Misquitta and K. Szalewicz, “Intermolecular forces from asymptotically corrected density functional description of monomers.” Chem. Phys. Lett. **357**, 301–306 (2002).
- ⁵¹A. J. Misquitta, B. Jeziorski, and K. Szalewicz, “Dispersion Energy from Density-Functional Theory Description of Monomers,” Phys. Rev. Lett. **91**, 033201 (2003).
- ⁵²A. J. Misquitta and K. Szalewicz, “Symmetry-adapted perturbation-theory calculations of intermolecular forces employing density-functional description of monomers.” J. Chem. Phys. **122**, 214109 (2005).
- ⁵³A. Hesselmann and G. Jansen, “First-order intermolecular interaction energies from Kohn-Sham orbitals.” Chem. Phys. Lett. **357**, 464–470 (2002).
- ⁵⁴A. Hesselmann, G. Jansen, and M. Schütz, “Density-functional theory-symmetry-adapted intermolecular perturbation theory with density fitting: A new efficient method to study intermolecular interaction energies.” J. Chem. Phys. **122**, 014103 (2004).
- ⁵⁵A. Hesselmann and G. Jansen, “Intermolecular induction and exchange-induction energies from coupled-perturbed Kohn-Sham density functional theory.” Chem. Phys. Lett. **362**, 319–325 (2002).
- ⁵⁶A. Hesselmann and G. Jansen, “Intermolecular dispersion energies from time-dependent density functional theory,” Chem. Phys. Lett. **367**, 778–784 (2003).
- ⁵⁷R. M. Parrish, K. C. Thompson, and T. J. Martínez, “Large-Scale Functional Group Symmetry-Adapted Perturbation Theory on Graphical Processing Units.” J. Chem. Theory Comput. **14**, 1737–1753 (2018).
- ⁵⁸J. B. Schriber, D. A. Sirianni, D. G. A. Smith, L. A. Burns, D. Sitkoff, D. L. Cheney, and C. D. Sherrill, “Optimized damping parameters for empirical dispersion corrections to symmetry-adapted perturbation theory.” J. Chem. Phys. **154**, 234107 (2021).
- ⁵⁹A. M. Wallace and C. D. Sherrill, “Optimization of damping function parameters for -D3 and -D4 dispersion models for Hartree–Fock based symmetry-adapted perturbation theory.” J. Chem. Phys. **161**, 114115 (2024).
- ⁶⁰A. Hesselmann, “Comparison of intermolecular interaction energies from SAPT and DFT including empirical dispersion contributions.” J. Phys. Chem. A **115**, 11321–11330 (2011).
- ⁶¹R. Sedlak and J. Řezáč, “Empirical D3 dispersion as a replacement for ab initio dispersion terms in density functional theory-based symmetry-adapted perturbation theory.” J. Chem. Theory Comput. **13**, 1638–1646 (2017).
- ⁶²K. U. Lao and J. M. Herbert, “Accurate intermolecular interactions at dramatically reduced cost: XPol plus SAPT with empirical dispersion.” J. Phys. Chem. Lett. **3**, 3241–3248 (2012).
- ⁶³K. U. Lao and J. M. Herbert, “Accurate and efficient quantum chemistry calculations for noncovalent interactions in many-body systems: The XS-APT family of methods.” J. Phys. Chem. A **119**, 235–252 (2015).
- ⁶⁴K. Carter-Fenk, K. U. Lao, and J. M. Herbert, “Predicting and Understanding Non-Covalent Interactions Using Novel Forms of Symmetry-Adapted Perturbation Theory.” Acc. Chem. Res. **54**, 3679–3690 (2021).
- ⁶⁵M. Gray and J. M. Herbert, “Comprehensive Basis-Set Testing of Extended Symmetry-Adapted Perturbation Theory and Assessment of Mixed-Basis Combinations to Reduce Cost.” J. Chem. Theor. Comput. **18**, 2308–2330 (2022).
- ⁶⁶C. Villot and K. U. Lao, “*Ab Initio* dispersion potentials based on physics-based functional forms with machine learning.” J. Chem. Phys. **160**, 184103 (2024).
- ⁶⁷C. S. Glick, A. Alenaizan, D. L. Cheney, C. E. Cavender, and C. D. Sherrill, “Electrostatically embedded symmetry-adapted perturbation theory,” (2024).
- ⁶⁸A. L. L. East and W. D. Allen, “The heat of formation of NCO.” J. Chem. Phys. **99**, 4638–4650 (1993).
- ⁶⁹A. G. Császár, W. D. Allen, and H. F. Schaefer, “In pursuit of the *ab initio* limit for conformational energy prototypes.” J. Chem. Phys. **108**, 9751–9764 (1998).
- ⁷⁰E. G. Hohenstein and C. D. Sherrill, “Density fitting of intramonomer correlation effects in symmetry-adapted perturbation theory.” J. Chem. Phys. **133**, 014101 (2010).
- ⁷¹E. G. Hohenstein and C. D. Sherrill, “Density fitting and Cholesky decomposition approximations in symmetry-adapted perturbation theory: Implementation and application to probe the nature of *pi-pi* interactions in linear acenes.” J. Chem. Phys. **132**, 184111 (2010).
- ⁷²R. M. Parrish, E. G. Hohenstein, and C. D. Sherrill, “Tractability gains in symmetry-adapted perturbation theory including coupled double excitations: CCD+ST(CCD) dispersion with natural orbital truncations.” J. Chem. Phys. **139**, 174102 (2013).
- ⁷³E. G. Hohenstein, *Implementation and applications of density-fitted symmetry-adapted perturbation theory*, Ph.D. thesis, Georgia Institute of Technology, Atlanta, GA (2011).
- ⁷⁴D. G. A. Smith, L. A. Burns, A. C. Simmonett, R. M. Parrish, M. C. Schieber, R. Galvelis, P. Kraus, H. Kruse, R. Di Remigio, A. Alenaizan, A. M. James, S. Lehtola, J. P. Misiewicz, M. Scheurer, R. A. Shaw, J. B. Schriber, Y. Xie, Z. L. Glick, D. A. Sirianni, J. S. O’Brien, J. M. Waldrop, A. Kumar, E. G. Hohenstein, B. P. Pritchard, B. R. Brooks, H. F. Schaefer, A. Y. Sokolov, K. Patkowski, A. E. DePrince, U. Bozkaya, R. A. King, F. A. Evangelista, J. M. Turney, T. D. Crawford, and C. D. Sherrill, “Psi4 1.4: Open-source software for high-throughput quantum chemistry.” J. Chem. Phys. **152**, 184108 (2020).
- ⁷⁵B. Jeziorski, R. Moszynski, A. Ratkiewicz, S. Rybak, and K. Szalewicz, “SAPT: A program for many-body symmetry-adapted perturbation theory calculations of intermolecular interaction energies,” in *Methods and Techniques in Computational Chemistry: METECC94*, Vol. B (Medium-Size Systems), edited by E. Clementi (STEF, Cagliari, 1993) p. 79.
- ⁷⁶K. Szalewicz and B. Jeziorski, in *Molecular Interactions: From van der Waals to Strongly Bound Complexes* (Wiley, 1997) Chap. Symmetry-adapted perturbation theory of in- termolecular interactions, p. 3.
- ⁷⁷K. Patkowski, K. Szalewicz, and B. Jeziorski, “Third-order interactions in symmetry-adapted perturbation theory.” J. Chem. Phys. **125**, 154107 (2006).
- ⁷⁸K. Patkowski, K. Szalewicz, and B. Jeziorski, “Orbital relaxation and the third-order induction energy in symmetry-adapted perurbation theory.” Theor. Chem. Acc. **127**, 211–221 (2010).

- ⁷⁹R. Schaeffer and G. Jansen, "Single-determinant-based symmetry-adapted perturbation theory without single-exchange approximation," *Mol. Phys.* **111**, 2570–2584 (2013).
- ⁸⁰B. W. Bakr and C. D. Sherrill, "Analysis of transition state stabilization by non-covalent interactions in the Houk-List model of organocatalyzed intermolecular Aldol additions using functional-group symmetry-adapted perturbation theory," *Phys. Chem. Chem. Phys.* **18**, 10297–10308 (2016).
- ⁸¹B. W. Bakr and C. D. Sherrill, "Analysis of transition state stabilization by non-covalent interactions in organocatalysis: Application of atomic and functional-group partitioned symmetry-adapted perturbation theory to the addition of organoboron reagents to fluoroketones," *Phys. Chem. Chem. Phys.* **20**, 18241–18251 (2018).
- ⁸²A. J. Misquitta, R. Bukowski, and K. Szalewicz, "Spectra of Ar–CO₂ from ab initio potential energy surfaces," *J. Chem. Phys.* **112**, 5308 (2000).
- ⁸³A. J. Sadlej, "Long range induction and dispersion interactions between hartree–fock subsystems," *Mol. Phys.* **39**, 1249–1264 (1980).
- ⁸⁴R. Moszynski, B. Jeziorski, S. Rybak, K. Szalewicz, and H. L. Williams, "Many-body theory of exchange effects in intermolecular interactions. density matrix approach and applications to He–F[−], He–HF, H₂–HF, and Ar–H₂ dimers," *J. Chem. Phys.* **100**, 5080–5092 (1994).
- ⁸⁵E. G. Hohenstein and C. D. Sherrill, "Wavefunction methods for noncovalent interactions," *WIREs Comput. Mol. Sci.* **2**, 304–326 (2012).
- ⁸⁶E. G. Hohenstein, H. M. Jaeger, E. J. Carroll, G. S. Tschumper, and C. D. Sherrill, "Accurate interaction energies for problematic dispersion-bound complexes: Homogeneous dimers of NCCN, P₂, and PCCP," *J. Chem. Theory Comput.* **7**, 2842–2851 (2011).
- ⁸⁷M. Pitoňák and A. Hesselmann, "Accurate Intermolecular Interaction Energies from a Combination of MP2 and TDDFT Response Theory," *J. Chem. Theory Comput.* **6**, 168–178 (2010).
- ⁸⁸R. Moszynski, B. Jeziorski, and K. Szalewicz, "Møller–Plesset expansion of the dispersion energy in the ring approximation," *Int. J. Quant. Chem.* **45**, 409–431 (1993).
- ⁸⁹L. A. Burns, J. C. Faver, Z. Zheng, M. S. Marshall, D. G. A. Smith, K. Vanommeslaeghe, A. D. MacKerell Jr., K. M. Merz Jr., and C. D. Sherrill, "The BioFragment Database (BFD_b): An open-data platform for computational chemistry analysis of noncovalent interactions," *J. Chem. Phys.* **147**, 161727 (2017).
- ⁹⁰D. G. A. Smith, L. A. Burns, K. Patkowski, and C. D. Sherrill, "Revised Damping Parameters for the D3 Dispersion Correction to Density Functional Theory," *J. Phys. Chem. Lett.* **7**, 2197–2203 (2016).
- ⁹¹J. Řezáč, K. E. Riley, and P. Hobza, "S66: A Well-balanced Database of Benchmark Interaction Energies Relevant to Biomolecular Structures," *J. Chem. Theor. Comput.* **7**, 2427–2438 (2011).
- ⁹²K. S. Thanthiripalage, E. G. Hohenstein, L. A. Burns, and C. D. Sherrill, "Assessment of the Performance of DFT and DFT-D Methods for Describing Distance Dependence of Hydrogen-Bonded Interactions," *J. Chem. Theor. Comput.* **7**, 88–96 (2011).
- ⁹³M. S. Marshall, L. A. Burns, and C. D. Sherrill, "Basis set convergence of the coupled-cluster correction, $\delta(\text{MP}2)(\text{CCSD(T)})$: best practices for benchmarking non-covalent interactions and the attendant revision of the S22, NBC10, HBC6, and HSG databases," *J. Chem. Phys.* **135**, 194102 (2011).
- ⁹⁴L. A. Burns, A. Vázquez-Mayagoitia, B. G. Sumpter, and C. D. Sherrill, "Density-functional approaches to noncovalent interactions: a comparison of dispersion corrections (DFT-D), exchange-hole dipole moment (XDM) theory, and specialized functionals," *J. Chem. Phys.* **134**, 084107 (2011).
- ⁹⁵J. Řezáč, K. E. Riley, and P. Hobza, "Benchmark Calculations of Noncovalent Interactions of Halogenated Molecules," *J. Chem. Theor. Comput.* **8**, 4285–4292 (2012).
- ⁹⁶K. U. Lao, R. Schäffer, G. Jansen, and J. M. Herbert, "Accurate description of intermolecular interactions involving ions using symmetry-adapted perturbation theory," *J. Chem. Theor. Comput.* **11**, 2473–2486 (2015).
- ⁹⁷E. Papajak, J. Zheng, X. Xu, H. R. Leverenz, and D. G. Truhlar, "Perspectives on basis sets beautiful: Seasonal plantings of diffuse basis functions," *J. Chem. Theory Comput.* **7**, 3027–3034 (2011).
- ⁹⁸S. Zahn, D. R. MacFarlane, and E. I. Izgorodina, "Assessment of Kohn–Sham density functional theory and Møller–Plesset perturbation theory for ionic liquids," *Phys. Chem. Chem. Phys.* **15**, 13664–13675 (2013).
- ⁹⁹S. F. Boys and F. Bernardi, "The calculation of small molecular interactions by the differences of separate total energies. Some procedures with reduced errors," *Mol. Phys.* **19**, 553–566 (1970).
- ¹⁰⁰K. Patkowski, "Chapter One - Benchmark Databases of Intermolecular Interaction Energies: Design, Construction, and Significance," in *Annual Reports in Computational Chemistry*, edited by D. A. Dixon (Elsevier, 2017) pp. 3–91.
- ¹⁰¹A. Halkier, T. Helgaker, P. Jørgensen, W. Klopper, H. Koch, J. Olsen, and A. K. Wilson, "Basis-set convergence in correlated calculations on Ne, N₂, and H₂O," *Chem. Phys. Lett.* **286**, 243–252 (1998).
- ¹⁰²L. A. Burns, M. S. Marshall, and C. D. Sherrill, "Comparing Counterpoise-Corrected, Uncorrected, and Averaged Binding Energies for Benchmarking Noncovalent Interactions," *J. Chem. Theor. Comput.* **10**, 49–57 (2014).
- ¹⁰³G. Chałasiński, B. Jeziorski, J. Andzelm, and K. Szalewicz, "On the multipole structure of exchange dispersion energy in the interaction of two helium atoms," *Mol. Phys.* **33**, 971–977 (1977).
- ¹⁰⁴M. Gutowski, J. Verbeek, J. H. van Lenthe, and G. Chałasiński, "The impact of higher polarization functions of second-order dispersion energy, partial wave expansion and damping phenomenon for He₂," *Chem. Phys.* **111**, 271–283 (1987).
- ¹⁰⁵S. Rybak, K. Szalewicz, B. Jeziorski, and M. Jaszunski, "Intraatomic correlation effects for the he–he dispersion and exchange–dispersion energies using explicitly correlated Gaussian geminals," *J. Chem. Phys.* **86**, 5652–5659 (1987).
- ¹⁰⁶H. L. Williams, T. Korona, R. Bukowski, B. Jeziorski, and K. Szalewicz, "Helium dimer potential from symmetry-adapted perturbation theory," *Chem. Phys. Lett.* **262**, 431–436 (1996).
- ¹⁰⁷T. Korona, H. L. Williams, R. Bukowski, B. Jeziorski, and K. Szalewicz, "Helium dimer potential from symmetry-adapted perturbation theory calculations using large Gaussian geminal and orbital basis sets," *J. Chem. Phys.* **106**, 5109–5122 (1997).